Electronic Supplementary Information

3-Keto-indazole derivatives exhibiting multi-coloured phosphorescence

Tetsuya Moriyama, Ryota Kobayashi, Takayuki Chiba, Shuji Okada, and Ryohei Yamakado*

Department of Organic Materials Science, Graduate School of Organic Materials Science, Yamagata University, Yonezawa 992–8510, Japan

Table of Contents

1. Synthetic procedures and spectroscopic data

General procedures. Starting materials were purchased from Kanto Chemical, TCI, and Sigma-Aldrich, and used without further purification unless otherwise stated. All reactions were performed under dry nitrogen atmosphere unless otherwise noted. ^{1}H and ^{13}C NMR spectra used in the characterization of products were recorded on a JEOL ECZ-600 (^{1}H: 600 MHz, ^{13}C: 150 MHz) spectrometer with chemical shifts (in ppm) relative to tetramethylsilane (^{1}H), solvent (^{13}C) as references. UV-visible absorption spectra were recorded on JASCO V-750ST spectrometer using a 10 mm quartz cell. Fluorescence spectra were recorded on JASCO FP-8600 fluorescence spectrometer. PL decay time was detected using a Hamamatsu C11367 Quantaurus-Tau fluorescence lifetime spectrometer with an excitation wavelength of 340 nm. The temperature dependence of PL spectra and PL decay time were measured using a liquid nitrogen cryostat system (UNISOKU CoolSpeK). Purifications with preparative gel permeation chromatography (GPC) were carried out on a Japan analytical industry LC-5060 system using tandem JAIGEL 2H, and 2.5H columns ($CHCl_3$ as an eluent, flow rate = 10 mL/min) equipped with an ultraviolet (UV) detector monitored at 254 nm. High-resolution electrospray ionization time-of-flight mass spectrometry (ESI-TOFMS) method using Waters Synapt G2 HDMS + Acquity or Bruker micrOTOFQ II ESI mass spectrometers in the positive ion mode. TLC analyses were carried out on aluminum sheets coated with silica gel 60 (Merck 5554). Column chromatography was performed on Mightysil Si60 (Kanto Chemical).

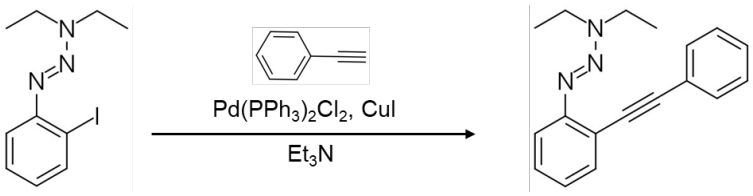

Synthesis of 1-{2-(1-ethynylphenyl)phenyl}-3,3-diethyltriaz-1-ene (TAz-Ph)

1-(2-Iodophenyl)-3,3-diethyltriaz-1-ene (362 mg, 1.20 mmol), $Pd(PPh_3)_2Cl_2$ (14.0 mg, 0.0240 mmol), and CuI (22.0 mg, 0.120 mmol) were added to a solution of ethynylbenzene (0.260 mL, 2.40 mmol) in Et_3N (5.00 mL) and the mixture was stirred under N_2 overnight at 60 °C. After the reaction was quenched with saturated NH_4Cl aq., CH_2Cl_2 was added. The combined organic layer was dried over Na_2SO_4, and the solvents were removed by a rotary evaporator. The residue was chromatographed over silica gel column (SiO_2; chloroform/hexane = 1/4) to afford **TAz-Ph** (248 mg, 75% yield) as a brown viscous liquid. R_f = 0.45 (chloroform/hexane = 1/4). ^{1}H-NMR (600 MHz, $CDCl_3$): δ (ppm) 7.53 (t, J = 9.3 Hz, 3H), 7.43 (d, J = 8.3 Hz, 1H), 7.33–7.24 (m, 4H), 7.09 (t, J = 7.6 Hz, 1H), 3.81 (q, J = 7.1 Hz, 4H), 1.32 (t, J = 7.2 Hz, 6H). ^{13}C-NMR (151 MHz, $CDCl_3$): δ (ppm) 152.5, 133.0, 131.6, 129.1, 128.4, 128.0, 124.9, 124.3, 118.3, 117.1, 93.4, 88.4, 49.3, 42.0, 14.9, 11.2.

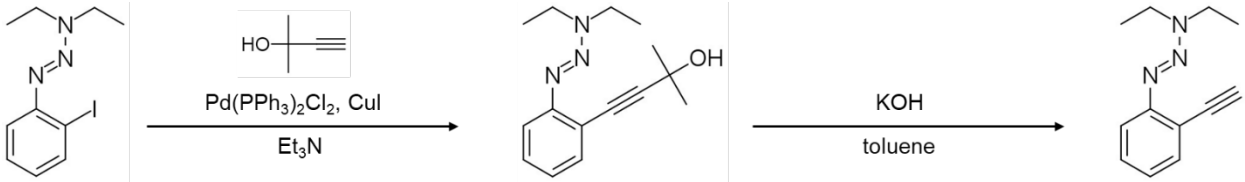

Synthesis of 1-(2-ethynylphenyl)-3,3-diethyltriaz-1-ene (TAz-H)

1-(2-Iodophenyl)-3,3-diethyltriaz-1-ene (1.52 g, 5.00 mmol), $Pd(PPh_3)_2Cl_2$ (350 mg, 0.500 mmol), and CuI (95.2 mg, 0.500 mmol) were added to a solution of 2-methyl-3-butyn-2-ol (505 mg, 6.00 mmol) in Et_3N (20.0 mL) and the mixture was stirred under N_2 overnight at 60 °C. After the reaction was quenched with saturated NH_4Cl aq., CH_2Cl_2 was added. The combined organic layer was dried over Na_2SO_4, and the solvents were removed by a rotary evaporator. The residue was chromatographed over silica gel column (SiO_2; EtOAc/CH_2Cl_2 = 1/4) to afford the product (752 mg, 58% yield) as a brown viscous liquid. R_f = 0.65 (EtOAc/CH_2Cl_2 = 1/4). ^{1}H-NMR (600 MHz, $CDCl_3$): δ (ppm) 7.40 (dd, J = 11.4, 7.9 Hz, 2H), 7.24 (t, J = 7.9 Hz, 1H), 7.04 (t, J = 7.2 Hz, 1H), 3.79 (q, J = 7.1 Hz, 4H), 2.19 (s, 1H), 1.62 (s, 6H), 1.31 (s, 6H). ^{13}C-NMR (151 MHz, $CDCl_3$): δ (ppm) 152.4, 133.0, 129.1, 124.8, 117.7, 116.9, 97.8, 80.8, 65.9, 49.3, 41.8, 31.7, 14.7, 11.2.

Obtained compound (752 mg, 2.90 mmol) was added to a solution of KOH (486 mg, 8.67 mmol) and the mixture was stirred at 100 °C for 4 hours. After the reaction was quenched with saturated NH_4Cl aq., hexane was added. The combined organic layer was dried over Na_2SO_4, and the solvents were removed by a rotary evaporator. The residue was chromatographed over silica gel column (SiO_2; EtOAc/hexane = 1/4) to afford **TAz-H** (129 mg, 22% yield) as a yellow viscous liquid. R_f = 0.60 (EtOAc/hexane = 1/4). ^{1}H-NMR (600 MHz, $CDCl_3$): δ (ppm) 7.49 (d, J = 7.6 Hz, 1H), 7.38 (d, J = 8.3 Hz, 1H), 7.27 (t, J = 6.9 Hz, 1H), 7.04 (t, J = 7.9 Hz, 1H), 3.77 (q, J = 7.1 Hz, 4H), 3.24 (s, 1H), 1.28 (s, 6H). ^{13}C-NMR (151 MHz, $CDCl_3$): δ (ppm) 153.2, 133.6, 129.4, 124.7, 117.2, 117.1, 82.2, 80.9, 49.1, 41.8, 14.6, 11.0.

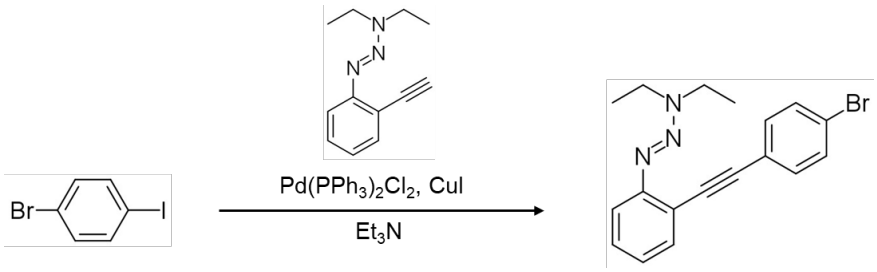

Synthesis of 1-{2-(4-bromophenyl)ethynylphenyl}-3,3-diethyltriaz-1-ene (TAz-BP)

1-Bromo-4-iodobenzen (141 mg, 0.500 mmol), $Pd(PPh_3)_2Cl_2$ (35.0 mg, 0.050 mmol), and CuI (9.50 mg, 0.050 mmol) were added to a solution of **TAz-H** (129 mg, 0.640 mmol) in Et_3N (5.00 mL) and the mixture was stirred under N_2 overnight at 60 °C. After the reaction was quenched with saturated NH_4Cl aq., CH_2Cl_2 was added. The combined organic layer was dried over Na_2SO_4, and the solvents were removed by a rotary evaporator. The residue was chromatographed over silica gel column (SiO_2; chloroform/hexane = 1/4) to afford **TAz-BP** (61 mg, 34% yield) as a yellow solid. R_f = 0.30 (chloroform/hexane = 1/4). ^{1}H-NMR (600 MHz, $CDCl_3$): δ (ppm) 7.51 (d, J = 6.9 Hz, 1H), 7.45 (d, J = 8.3 Hz, 2H), 7.43 (d, J = 8.3 Hz, 1H), 7.36 (d, J = 8.3 Hz, 2H), 7.28 (t, J = 7.2 Hz, 1H), 7.09 (t, J = 7.6 Hz, 1H), 3.81 (q, J = 7.1 Hz, 4H), 1.32 (s, 6H). ^{13}C-NMR (151 MHz, $CDCl_3$): δ (ppm) 152.6, 133.0, 132.9, 131.7, 129.4, 124.9, 123.3, 122.1, 117.9, 117.2, 92.3, 89.6, 49.4, 41.9, 14.8, 11.2.

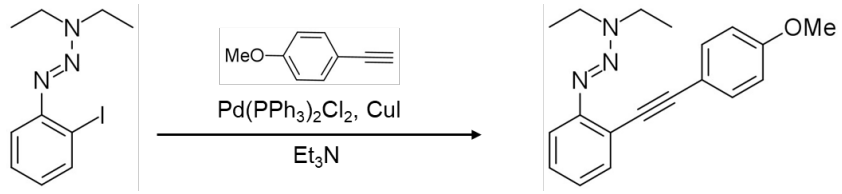

Synthesis of 1-{2-(4-methoxyphenyl)ethynylphenyl}-3,3-diethyltriaz-1-ene (TAz-MP)

1-(2-Iodophenyl)-3,3-diethyltriaz-1-ene (424 mg, 1.40 mmol), $Pd(PPh_3)_2Cl_2$ (5.00 mg, 0.00712 mmol), and CuI (13.0 mg, 0.0683 mmol) were added to a solution of 4-ethynylanisole (292 mg, 2.21 mmol) in Et_3N (15.0 mL) and the mixture was stirred under N_2 overnight at 60 °C. After the reaction was quenched with saturated NH_4Cl aq., CH_2Cl_2 was added. The combined organic layer was dried over Na_2SO_4, and the solvents were removed by a rotary evaporator. The residue was chromatographed over silica gel column (SiO_2; chloroform/hexane = 1/1) to afford **TAz-MP** (92 mg, 21% yield) as a yellow viscous liquid. R_f = 0.45 (chloroform/hexane = 1/1). ^{1}H-NMR (600 MHz, $CDCl_3$): δ (ppm) 7.51 (d, J = 6.9 Hz, 1H), 7.45 (d, J = 9.0 Hz, 2H), 7.41 (d, J = 8.3 Hz, 1H), 7.25 (d, J = 13.8 Hz, 1H), 7.08 (t, J = 7.9 Hz, 1H), 6.85 (d, J = 9.0 Hz, 2H), 3.80 (q, J = 7.1 Hz, 6H), 1.32 (t, J = 6.9 Hz, 6H). ^{13}C-NMR (151 MHz, $CDCl_3$): δ (ppm) 159.4, 152.3, 133.0, 132.8, 128.7, 125.1, 124.9, 124.7, 118.6, 117.1, 116.4, 114.0, 93.4, 86.9, 55.4, 49.3, 41.9, 14.7, 11.2.

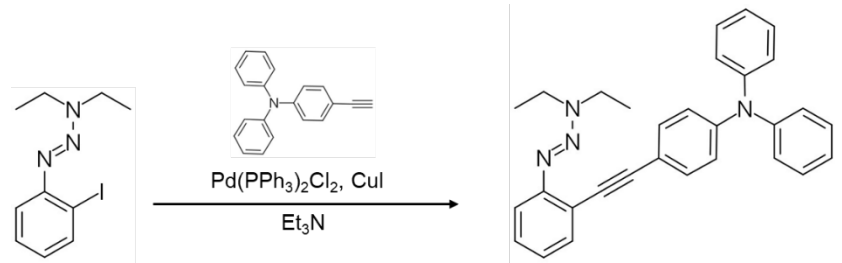

Synthesis of 1-{2-[4-(diphenylamino)phenyl]ethynylphenyl}-3,3-diethyltriaz-1-ene (TAz-TPA)

1-(2-Iodophenyl)-3,3-diethyltriaz-1-ene (160 mg, 0.528 mmol), $Pd(PPh_3)_2Cl_2$ (5.00 mg, 0.00712 mmol), and CuI (9.00 mg, 0.0473 mmol) were added to a solution of 4-ethynyl-*N*,*N*-diphenylaniline (289 mg, 1.07 mmol) in Et_3N (8.00 mL) and the mixture was stirred under N_2 overnight at 60 °C. After the reaction was quenched with saturated NH_4Cl aq., CH_2Cl_2 was added. The combined organic layer was dried over Na_2SO_4, and the solvents were removed by a rotary evaporator. The residue was chromatographed over silica gel column (SiO_2; EtOAc/hexane = 1/8) and was purified by recycling preparative GPC to afford **TAz-TPA** (78.0 mg, 33% yield) as a brown viscous liquid. R_f = 0.50 (EtOAc/hexane = 1/8). ^{1}H-NMR (600 MHz, $CDCl_3$): δ (ppm) 7.50 (d, J = 6.9 Hz, 1H), 7.41 (d, J = 7.6 Hz, 1H), 7.36 (d, J = 9.0 Hz, 2H), 7.26–7.19 (m, 5H), 7.10 (d, J = 7.6 Hz, 4H), 7.07–6.98 (m, 5H), 3.79 (q, J = 7.1 Hz, 4H), 1.30 (t, J = 7.2 Hz, 6H). ^{13}C-NMR (151 MHz, $CDCl_3$): δ (ppm) 152.2, 147.6, 147.4, 132.8, 132.5, 129.5, 128.7, 125.0, 124.8, 123.5, 122.5, 118.7, 118.6, 118.5, 117.4, 117.3, 117.0, 116.9, 93.7, 87.6, 49.2, 41.9, 14.7, 11.2.

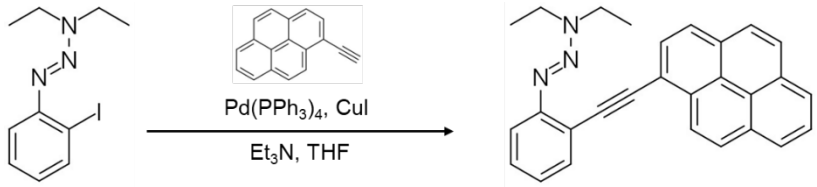

Synthesis of 1-{2-(1- ethynylpyrenyl)phenyl}-3,3-diethyltriaz-1-ene (TAz-Pyr)

1-(2-Iodophenyl)-3,3-diethyltriaz-1-ene (424 mg, 1.40 mmol), $Pd(PPh_3)_4$ (18.0 mg, 0.0150 mmol), and CuI (21.0 mg, 0.110 mmol) were added to a solution of 1-ethynylpyrene (634 mg, 2.80 mmol) in Et_3N (3.00 mL) and THF (3.00 mL), and the mixture was stirred under N_2 overnight at 70 °C. After the reaction was quenched with saturated NH_4Cl aq., CH_2Cl_2 was added. The combined organic layer was dried over Na_2SO_4, and the solvents were removed by a rotary evaporator. The residue was chromatographed over silica gel column (SiO_2; dichloromethane/hexane = 1/2) to afford **TAz-Pyr** (390 mg, 69% yield) as a yellow solid. R_f = 0.45 (dichloromethane/hexane = 1/2). ^{1}H-NMR (600 MHz, $CDCl_3$): δ (ppm) 8.81 (d, *J* = 9.6 Hz, 1H), 8.19–8.14 (m, 3H), 8.09 (dd, *J* = 8.6, 2.4 Hz, 2H), 8.05–7.97 (m, 3H), 7.73 (d, *J* = 9.0 Hz, 1H), 7.54 (d, *J* = 8.3 Hz, 1H), 7.33 (t, *J* = 6.9 Hz, 1H), 7.17 (t, *J* = 6.9 Hz, 1H), 4.05–3.75 (4H), 1.33 (t, *J* = 7.2 Hz, 6H). ^{13}C-NMR (151 MHz, $CDCl_3$): δ (ppm) 152.6, 133.3, 132.0, 131.5, 131.3, 131.1, 129.6, 129.3, 128.0, 127.9, 127.4, 126.3, 126.3, 125.5, 125.0, 124.7, 124.7, 124.5, 119.1, 118.5, 117.3, 94.4, 92.6, 49.2, 41.7, 14.7, 11.5.

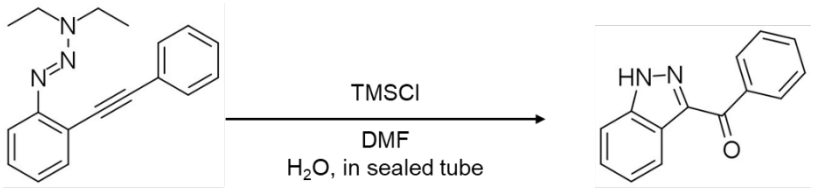

Synthesis of 3-(phenylcarbonyl)-1*H*-indazole (Ind-Ph)

TMSCl (190 μL, 1.50 mmol) was added to a solution of **TAz-Ph** (139 mg, 0.500 mmol) in DMF (8.8 mL) and a few drops of water. The mixture was stirred in a sealed tube at 60 °C for 24 h. The resulting mixture was extracted with CH_2Cl_2 and washed with water. The organic phase was dried over Na_2SO_4, and the solvents were removed under reduced pressure. The residue was purified by silica gel column chromatography (SiO_2; chloroform/hexane = 1/4 to EtOAc/hexane = 1/2) to afford **Ind-Ph** (21.1 mg, 19% yield) as an ochre solid. R_f = 0.50 (EtOAc /hexane = 1/2). ^{1}H-NMR (500 MHz, $CDCl_3$): δ (ppm) 10.78 (s, 1H), 8.48 (d, *J* = 8.3 Hz, 1H), 8.29 (dd, *J* = 8.3 Hz, 2H), 7.62 (t, *J* = 7.2 Hz, 1H), 7.54 (q, *J* = 8.0 Hz, 3H), 7.49 (t, *J* = 7.6 Hz, 1H), 7.39 (t, *J* = 7.9 Hz, 1H). ^{13}C NMR (151 MHz, $CDCl_3$): δ (ppm) 189.4, 143.8, 141.0, 138.1, 132.8, 130.6, 128.4, 127.9, 124.0, 123.6, 123.1, 110.1. ESI-TOF-MS: *m/z* (%intensity): 245.0685 (100). Calcd for $C_{14}H_{10}N_2ONa$ ($[M+Na]^+$): 245.0685.

Synthesis of 3-[(4-bromophenyl)carbonyl]-1*H*-indazole (Ind-BP)

TMSCl (64.8 μL, 0.510 mmol) was added to a solution of **TAz-BP** (61.0 mg, 0.170 mmol) in DMF (3.05 mL) and a few drops of water. The mixture was stirred in a sealed tube at 60 °C for 24 h. The resulting mixture was extracted with CH_2Cl_2 and washed with water. The organic phase was dried over Na_2SO_4, and the solvents were removed under reduced pressure. The residue was purified by silica gel column chromatography (SiO_2; EtOAc/hexane = 1/4) and recycle preparative GPC to afford **Ind-BP** (18.3 mg, 35% yield) as a white solid. R_f = 0.40 (EtOAc /hexane = 1/4). ^{1}H-NMR (600 MHz, $CDCl_3$): δ (ppm) 10.47 (s, 1H), 8.48 (d, J = 8.3 Hz, 1H), 8.22 (d, *J* = 9.0 Hz, 2H), 7.67 (d, *J* = 9.0 Hz, 2H), 7.60 (d, *J* = 9.0 Hz, 1H), 7.51 (t, *J* = 7.6 Hz, 1H), 7.41 (t, *J* = 7.2 Hz, 1H). ^{13}C NMR (151 MHz, $CDCl_3$): δ (ppm) 188.0, 143.7, 140.9, 136.7, 132.2, 131.7, 128.0, 127.9, 124.2, 123.6, 123.2, 110.0. ESI-TOF-MS: *m/z* (%intensity): 300.9971 (100). Calcd for $C_{14}H_{10}BrN_2O$ ($[M+H]^+$): 300.9977.

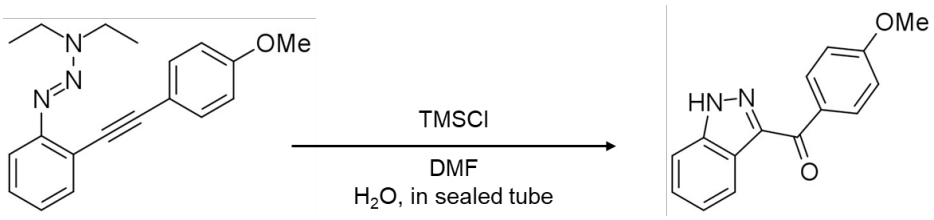

Synthesis of 3-[(4-methoxyphenyl)carbonyl]-1*H*-indazole (Ind-MP)

TMSCl (76.1 μL, 0.600 mmol) was added to a solution of **TAz-MP** (61.5 mg, 0.200 mmol) in DMF (3.50 mL) and a few drops of water. The mixture was stirred in a sealed tube at 60 °C for 24 h. The resulting mixture was extracted with CH_2Cl_2 and washed with water. The organic phase was dried over Na_2SO_4, and the solvents were removed under reduced pressure. The residue was purified by silica gel column chromatography (SiO_2; EtOAc/hexane = 1/2) and recrystallization (chloroform/hexane = 1/1) to afford **Ind-MP** (31 mg, 61% yield) as a white solid. R_f = 0.40 (EtOAc /hexane = 1/2). ^{1}H-NMR (600 MHz, $CDCl_3$): δ (ppm) 10.42 (s, 1H), 8.47 (d, J = 8.3 Hz, 1H), 8.38 (d, J = 9.0 Hz, 2H), 7.58 (d, J = 8.3 Hz, 1H), 7.49 (t, J = 7.2 Hz, 1H), 7.38 (t, J = 7.2 Hz, 1H), 7.02 (d, J = 9.0 Hz, 2H), 3.91 (s, 3H). ^{13}C NMR (151 MHz, $CDCl_3$): δ (ppm) 187.9, 163.5, 144.0, 140.9, 133.0, 130.8, 127.6, 123.7, 123.6, 123.1, 113.7, 110.1, 55.6. ESI-TOF-MS: *m/z* (%intensity): 253.0972 (100). Calcd for $C_{15}H_{13}N_2O_2$ ($[M+H]^+$): 253.0977.

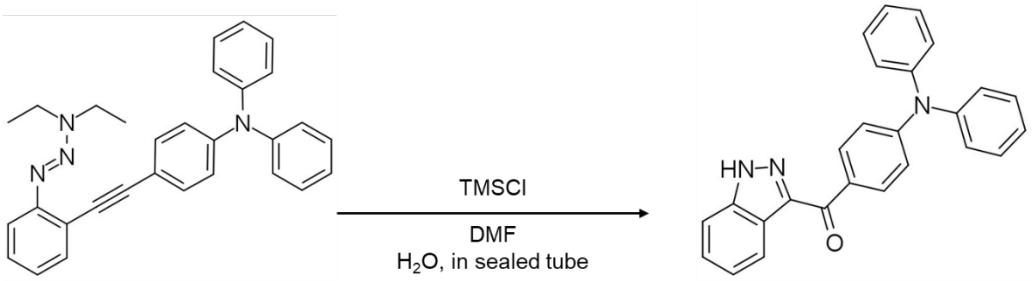

Synthesis of 3-[4-(diphenylamino)phenyl]carbonyl-1*H*-indazole (Ind-TPA)

TMSCl (76.1 μL, 0.600 mmol) were added to a solution of **TAz-TPA** (89.0 mg, 0.200 mmol) in DMF (3.50 mL) and a few drops of water. The mixture was stirred in a sealed tube at 60 °C for 24 h. The resulting mixture was extracted with CH_2Cl_2 and washed with water. The organic phase was dried over Na_2SO_4, and the solvents were removed under reduced pressure. The residue was purified by silica gel column chromatography (SiO_2; EtOAc) to afford **Ind-TPA** (66.2 mg, 85% yield) as a yellow solid. R_f = 0.40 (EtOAc /hexane = 1/4). ^{1}H-NMR (600 MHz, $CDCl_3$): δ (ppm) 10.38 (s, 1H), 8.47 (d, J = 8.3 Hz, 1H), 8.24 (d, J = 9.0 Hz, 2H), 7.57 (d, J = 9.0 Hz, 1H), 7.48 (t, J = 7.2 Hz, 1H), 7.37 (t, J = 7.6 Hz, 1H), 7.32 (t, J = 7.9 Hz, 4H), 7.19 (d, J = 7.2 Hz, 4H), 7.14 (t, J = 7.6 Hz, 2H), 7.07 (d, J = 9.0 Hz, 2H). ^{13}C NMR (151 MHz, $CDCl_3$): δ (ppm) 187.4, 152.2, 146.7, 144.0, 140.9, 132.4, 130.2, 129.7, 127.6, 126.1, 124.7, 123.6, 123.1, 119.8, 110.2. ESI-TOF-MS: *m/z* (%intensity): 412.1420 (100). Calcd for $C_{26}H_{19}N_3ONa$ ($[M+Na]^+$): 412.1420.

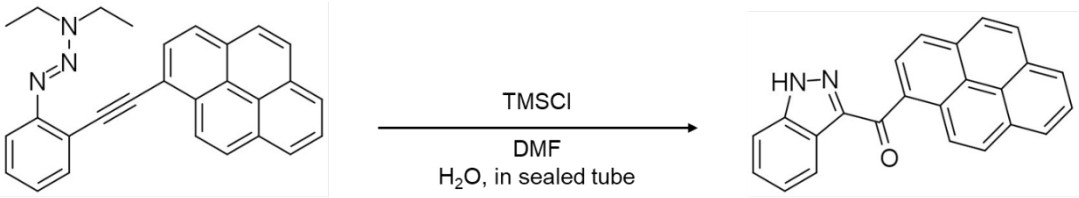

Synthesis of 3-(1-carbonylpyrenyl)-1*H*-indazole (Ind-Pyr)

TMSCl (76.1 μL, 0.600 mmol) was added to a solution of **TAz-Pyr** (80.5 mg, 0.200 mmol) in DMF (3.50 mL) and a few drops of water. The mixture was stirred in a sealed tube at 60 °C for 24 h. The resulting mixture was extracted with CH_2Cl_2 and washed with water. The organic phase was dried over Na_2SO_4, and the solvents were removed under reduced pressure. The residue was purified by silica gel column chromatography (SiO_2; chloroform/hexane = 1/4 to EtOAc/hexane = 1/2) to afford **Ind-Pyr** (29.6 mg, 43% yield) as a yellow solid. R_f = 0.40 (EtOAc /hexane = 1/2). ^{1}H-NMR (600 MHz, $CDCl_3$): δ (ppm) 10.41 (s, 1H), 8.58 (dd, J = 13.8, 9.0 Hz, 2H), 8.44 (d, J = 7.6 Hz, 1H), 8.27–8.23 (m, 3H), 8.19 (d, J = 9.0 Hz, 1H), 8.14 (d, J = 6.2 Hz, 2H), 8.06 (t, J = 7.6 Hz, 1H), 7.59 (d, J = 8.3 Hz, 1H), 7.54 (t, J = 7.6 Hz, 1H), 7.46 (t, J = 7.6 Hz, 1H). ESI-TOF-MS: *m/z* (%intensity): 369.0998 (100). Calcd for $C_{24}H_{14}N_2ONa$ ($[M+Na]^+$): 369.0998. Due to low solubility, ^{13}C-NMR could not be measured.

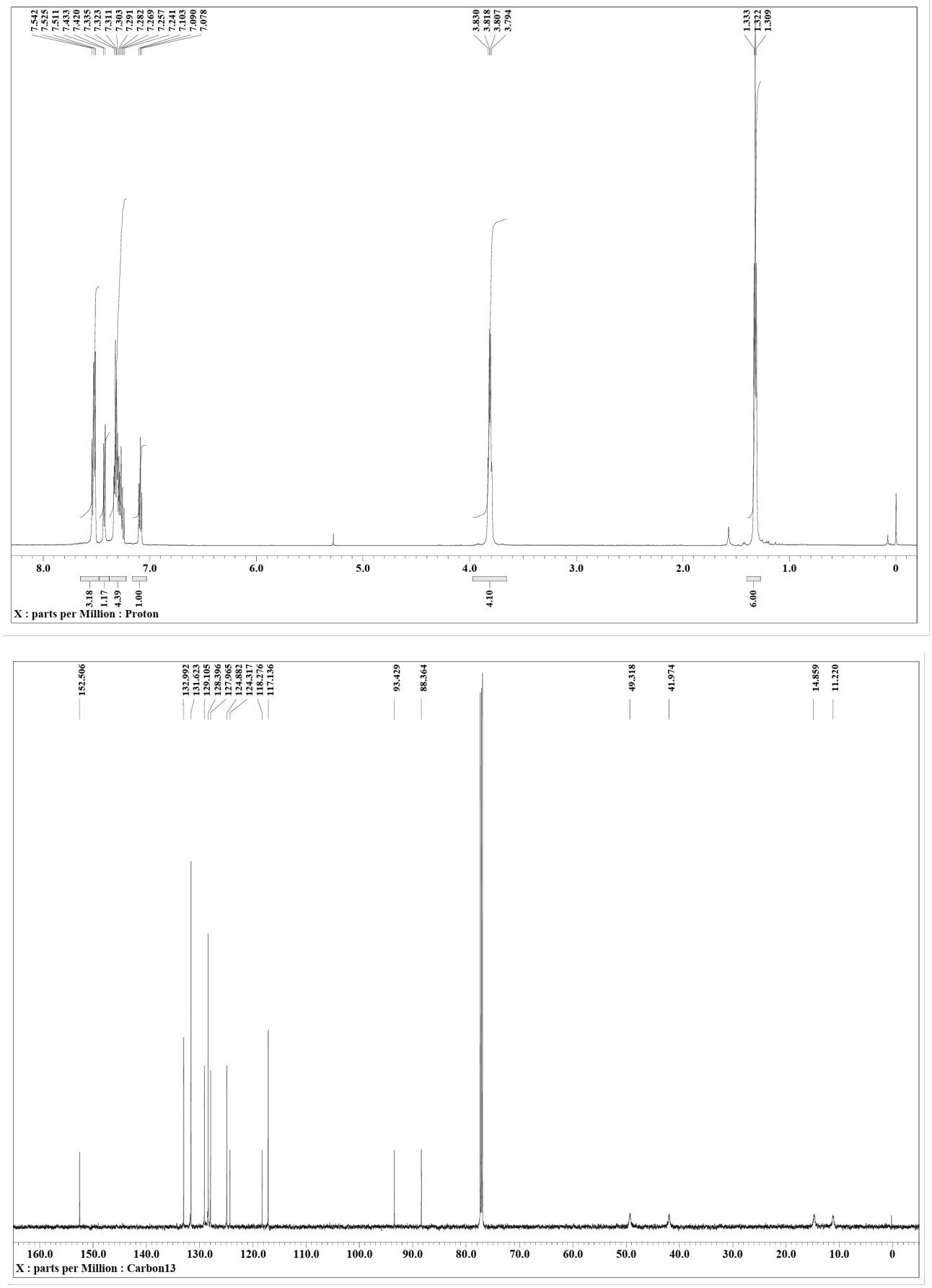

Fig. S1 ^{1}H (top) and ^{13}C (bottom) NMR spectra of **TAz-Ph** in $CDCl_3$ at 298 K.

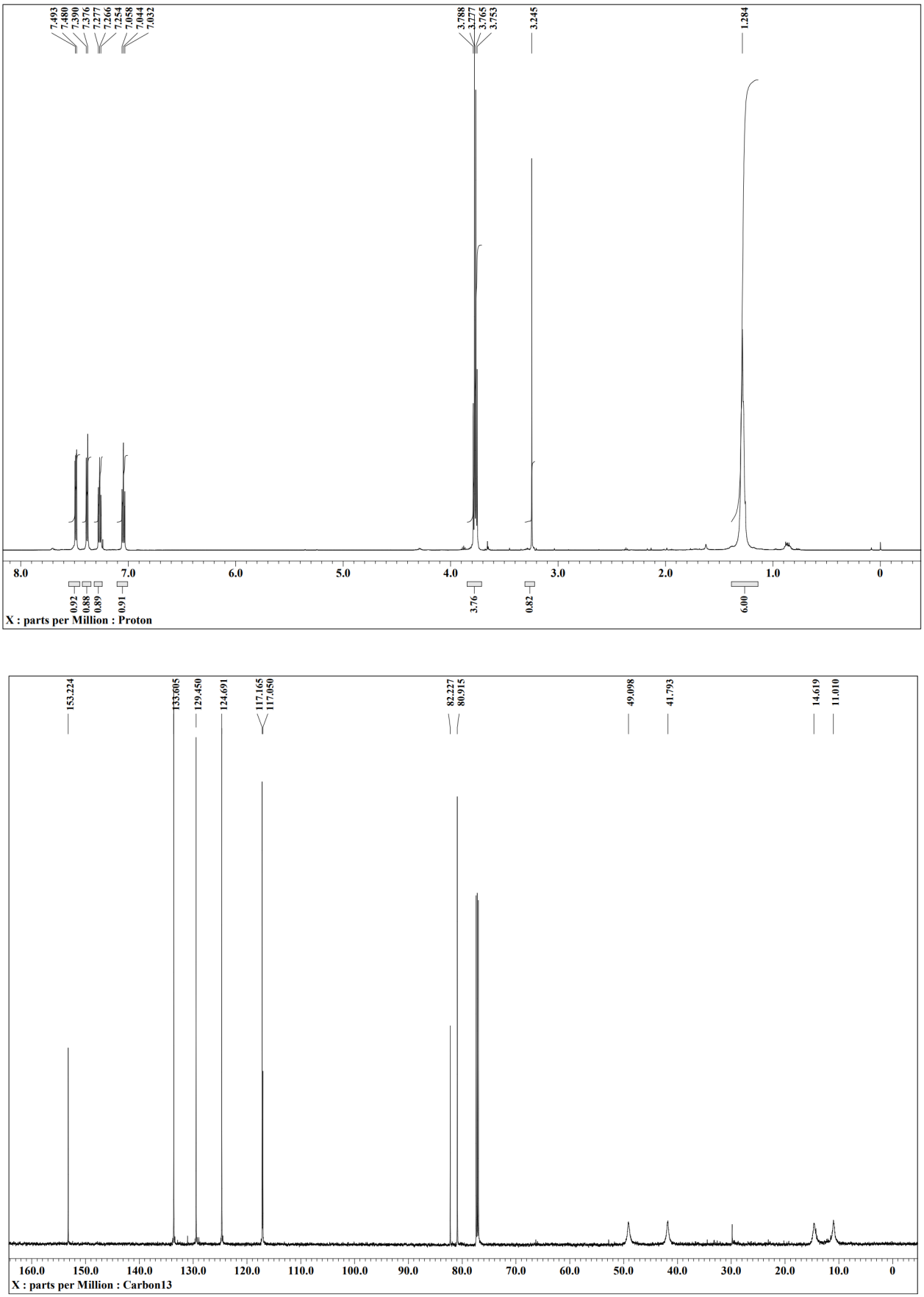

Fig. S2 ^{1}H (top) and ^{13}C (bottom) NMR spectra of **TAz-H** in $CDCl_3$ at 298 K.

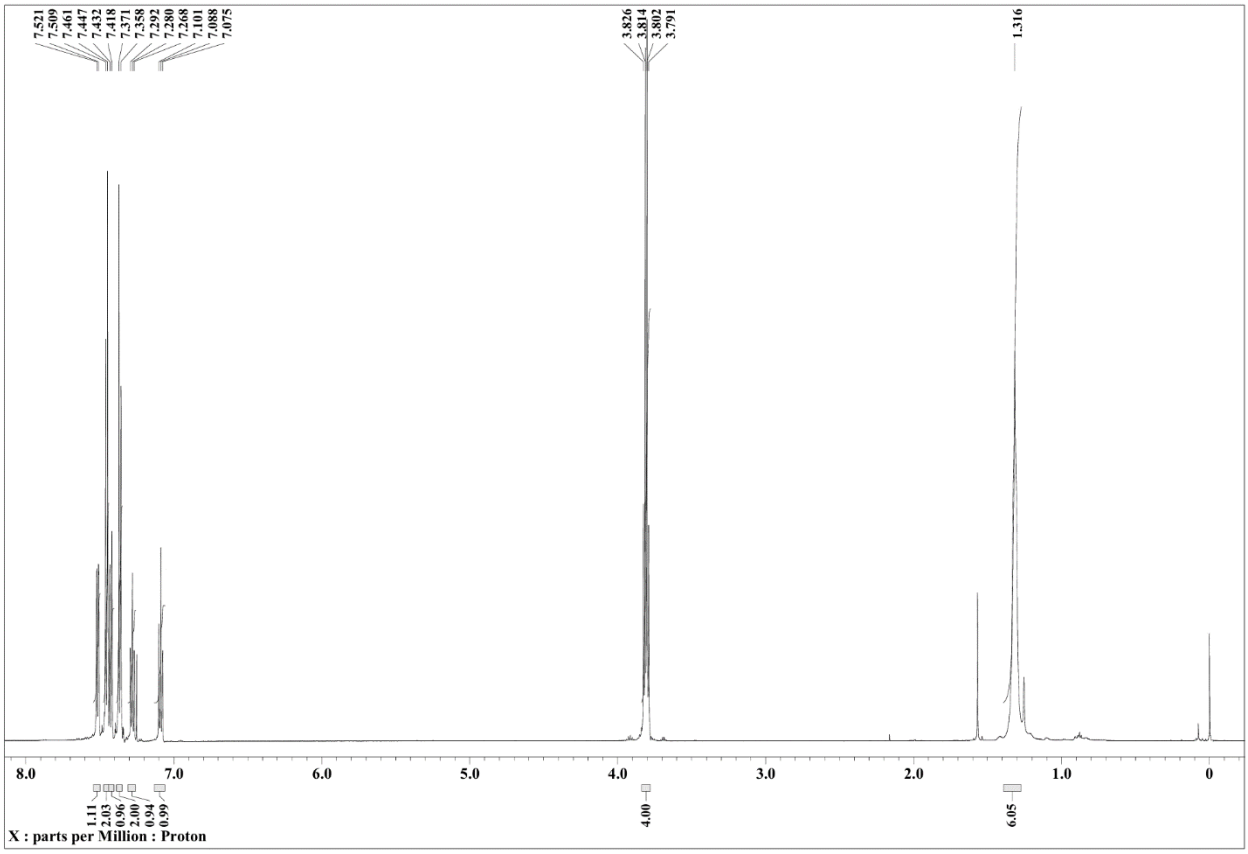

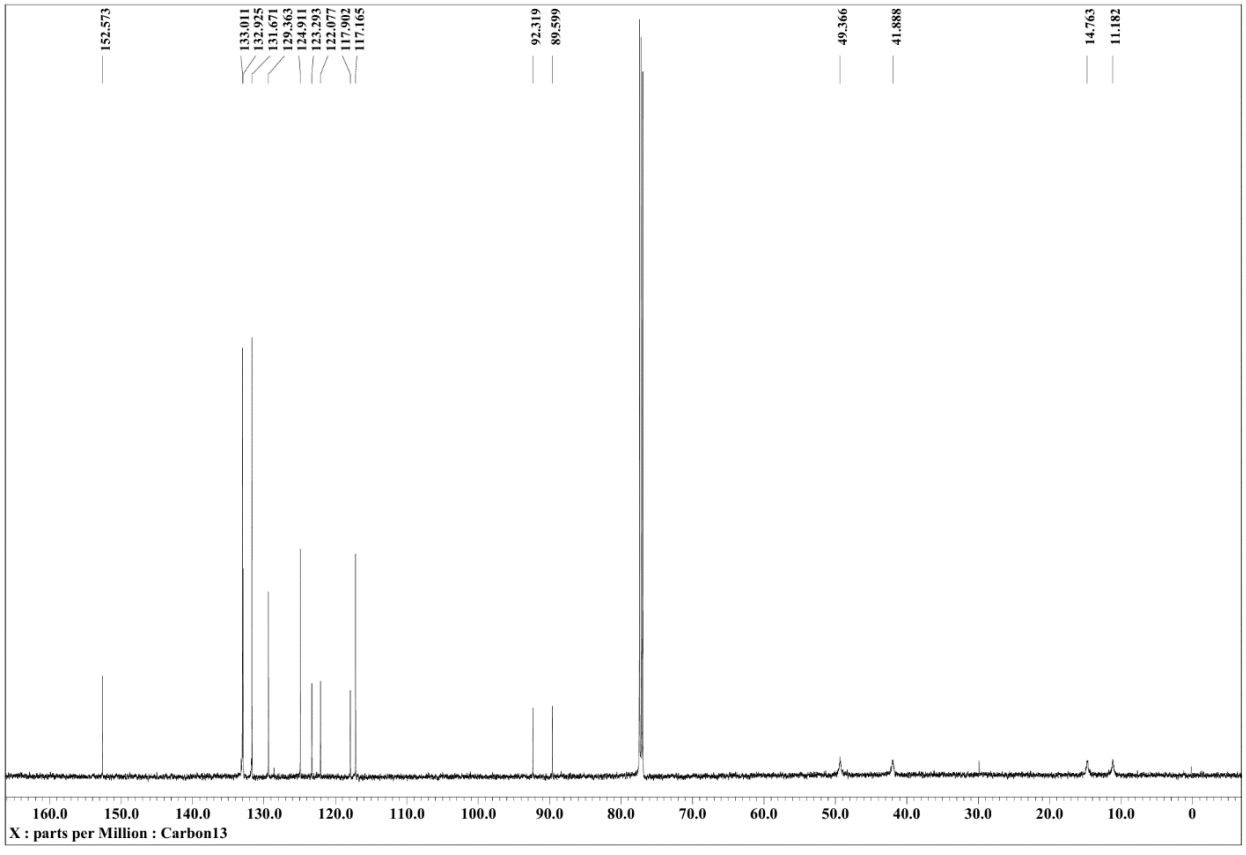

Fig. S3 ^{1}H (top) and ^{13}C (bottom) NMR spectra of **TAz-BP** in $CDCl_3$ at 298 K.

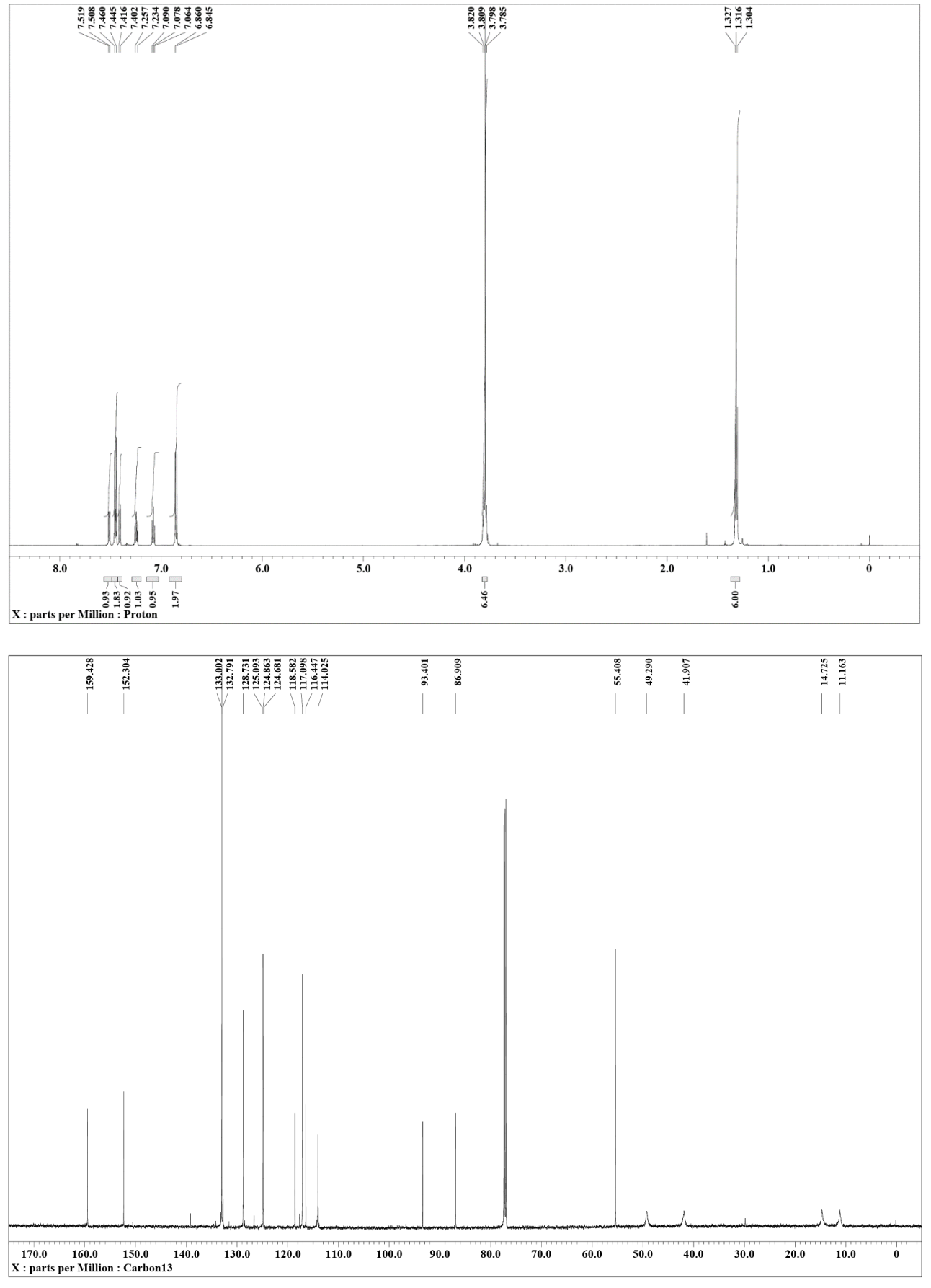

Fig. S4 ^{1}H (top) and ^{13}C (bottom) NMR spectra of **TAz-MP** in $CDCl_3$ at 298 K.

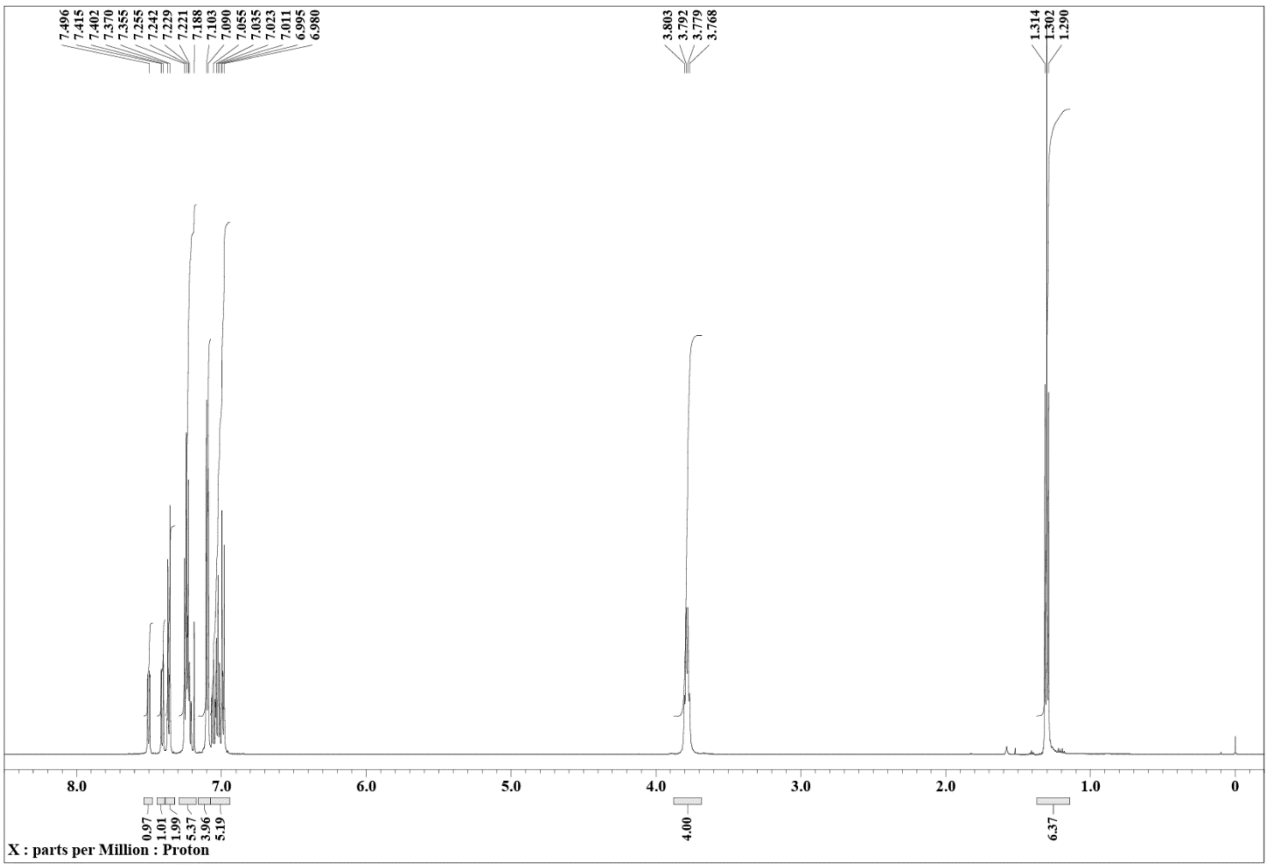

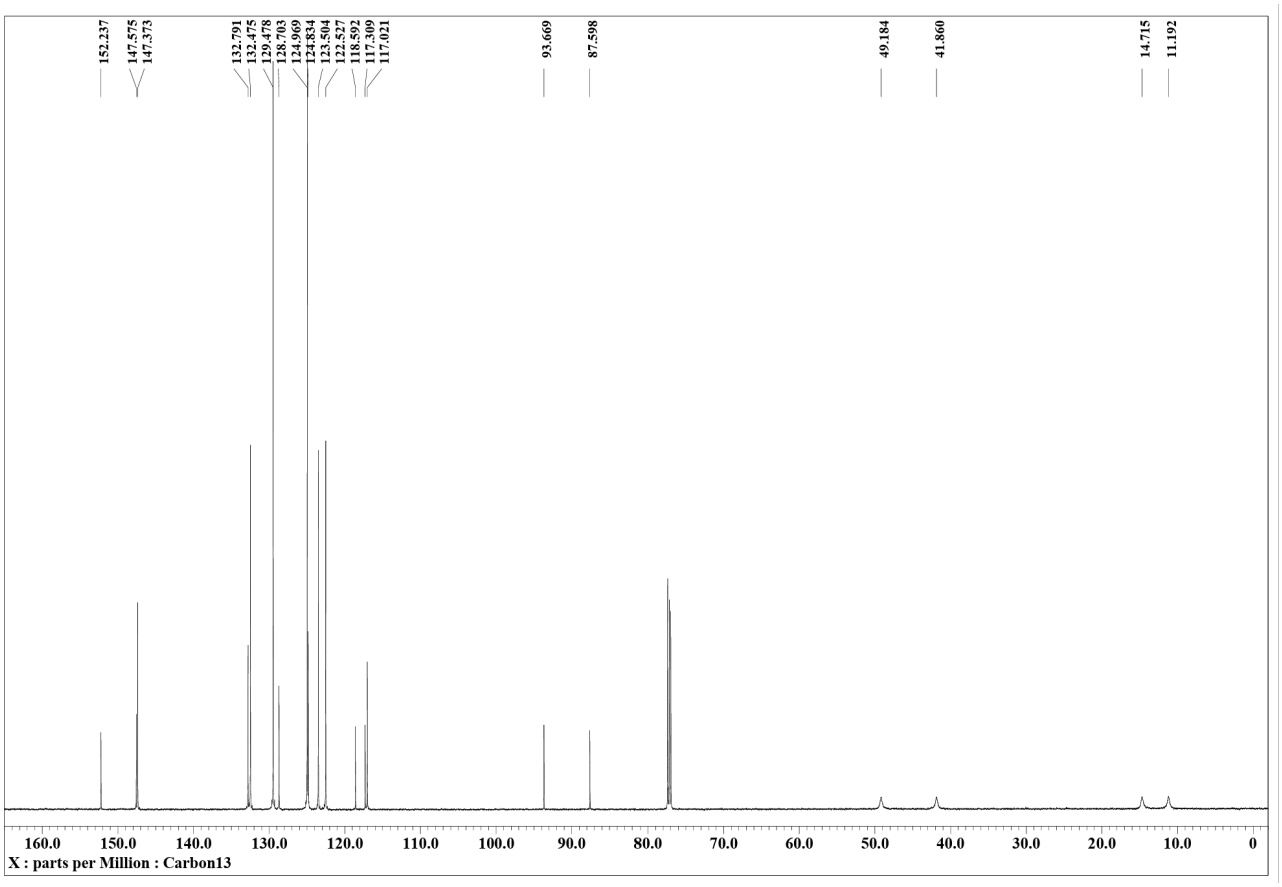

Fig. S5 ^{1}H (top) and ^{13}C (bottom) NMR spectra of **TAz-TPA** in $CDCl_3$ at 298 K.

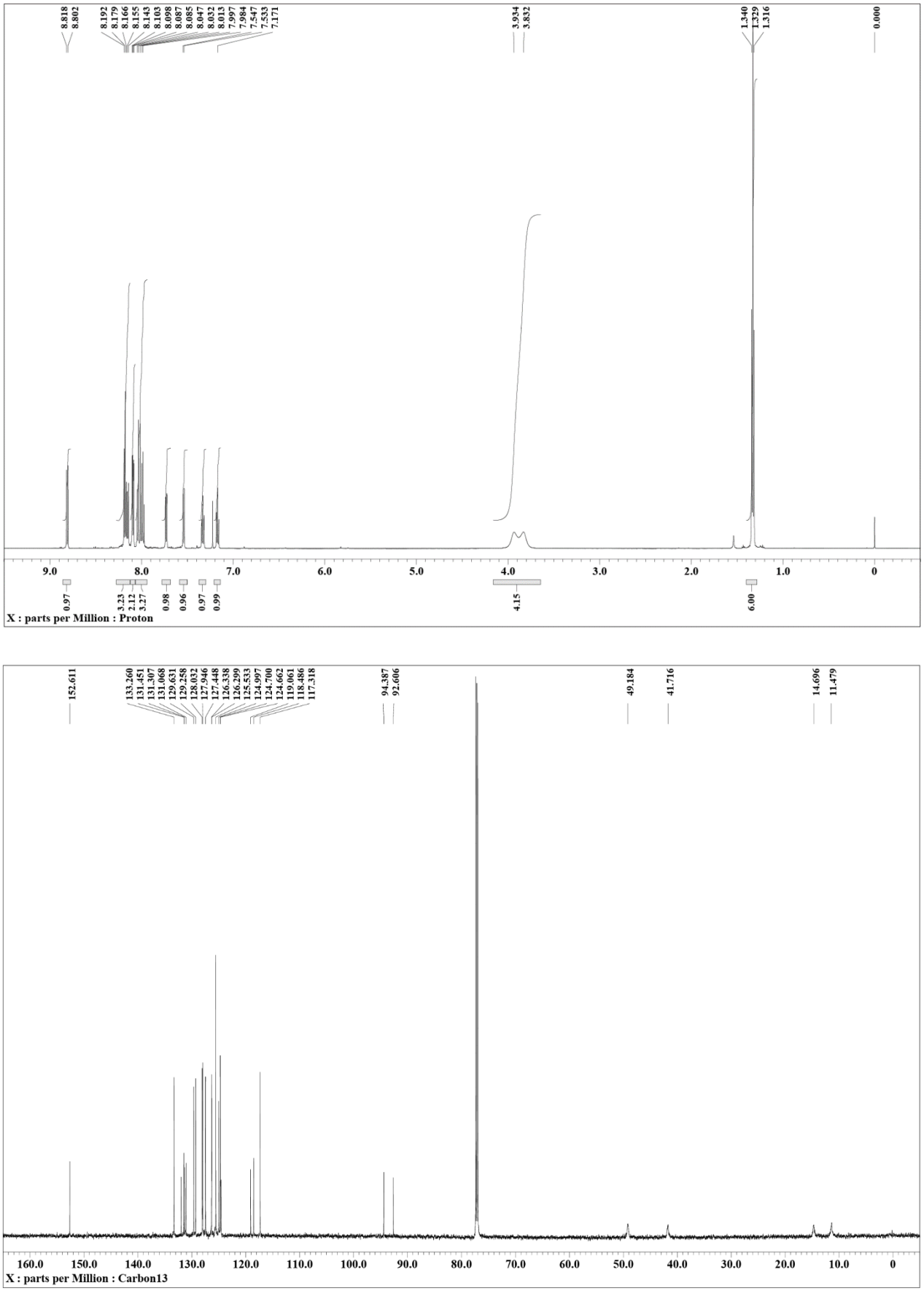

Fig. S6 ^{1}H (top) and ^{13}C (bottom) NMR spectra of **TAz-Pyr** in $CDCl_3$ at 298 K.

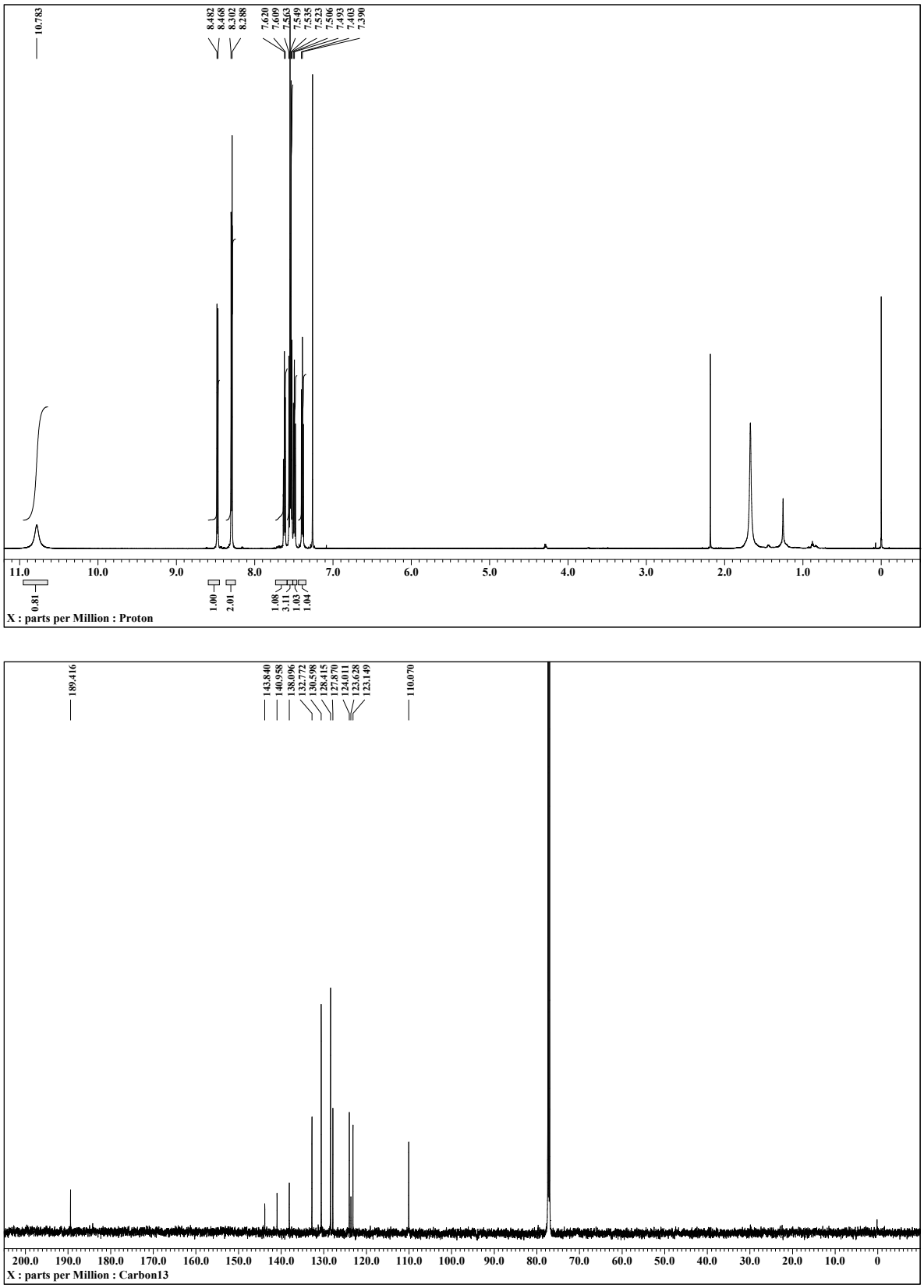

Fig. S7 ^{1}H (top) and ^{13}C (bottom) spectra of **Ind-Ph** in $CDCl_3$ at 298 K.

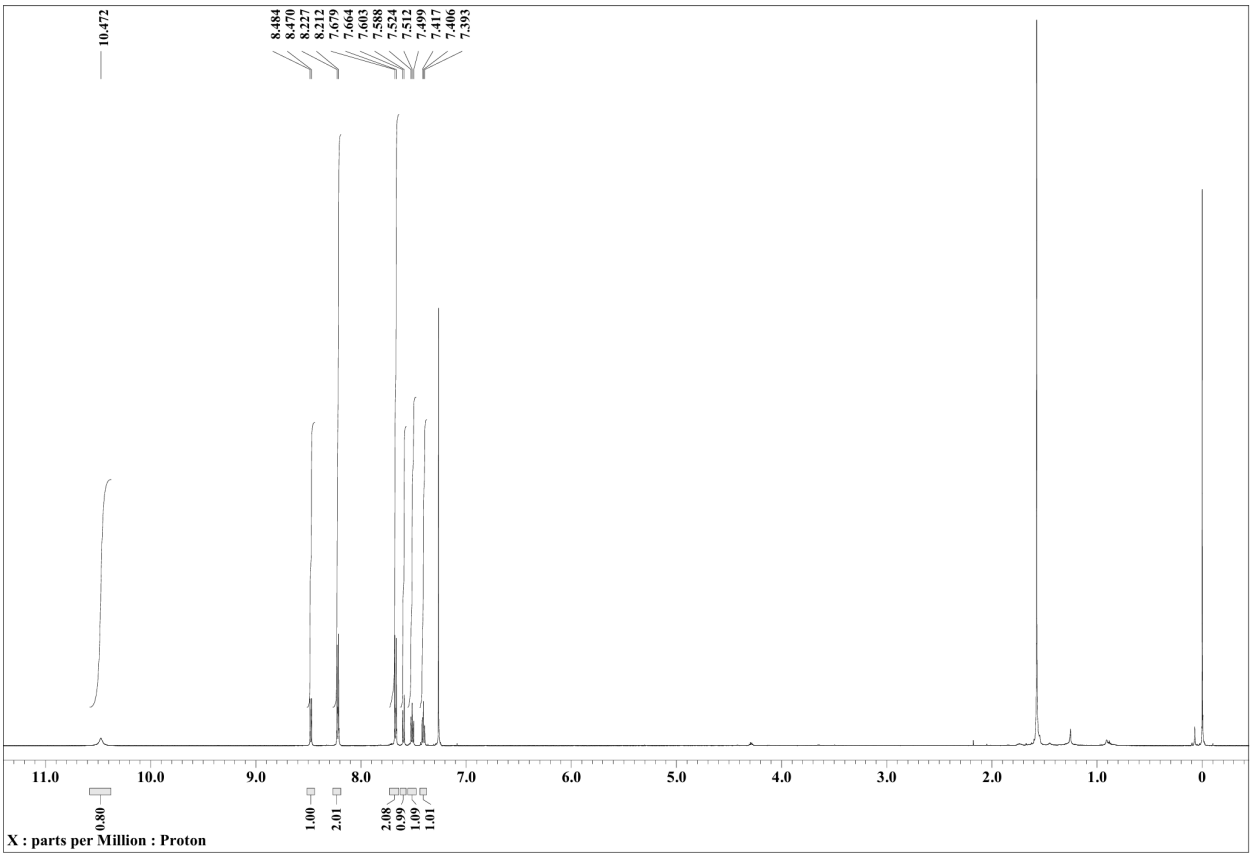

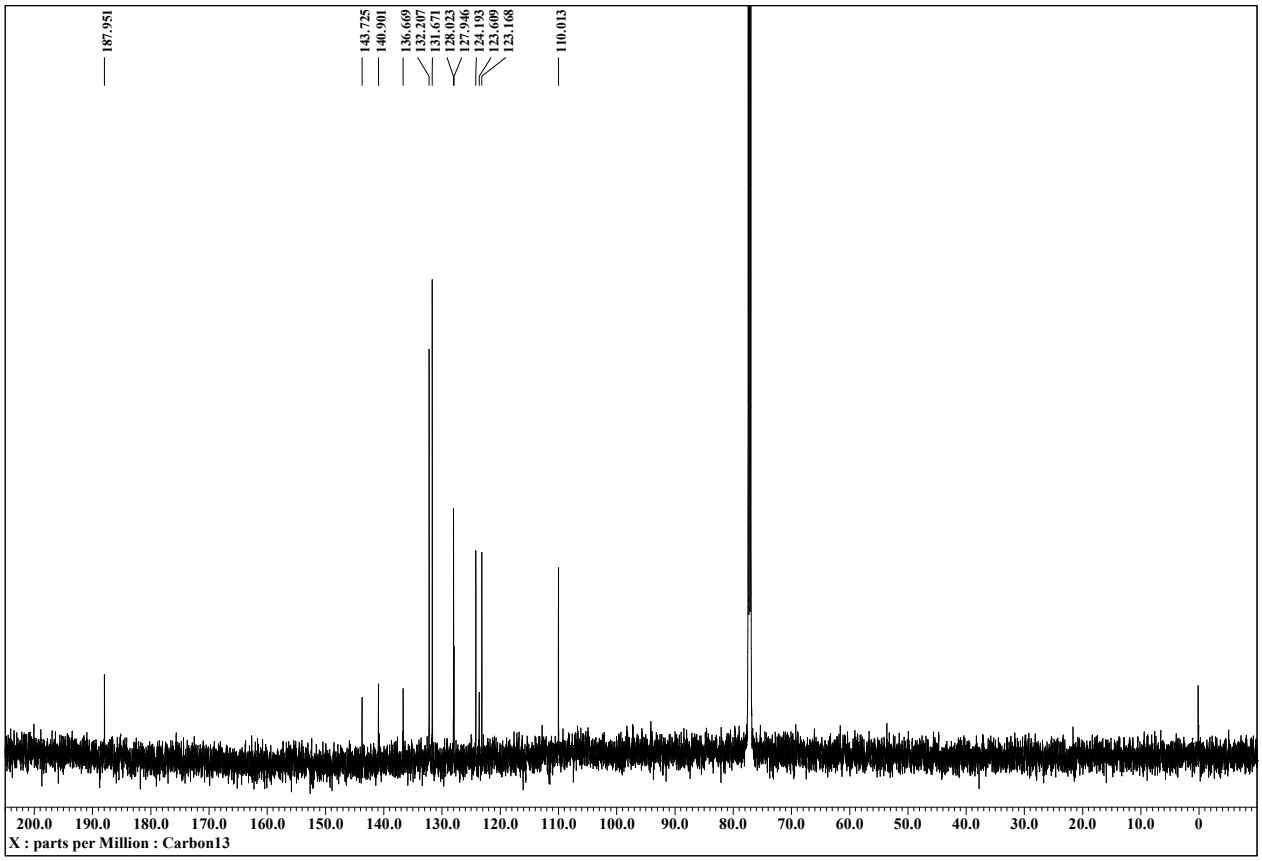

Fig. S8 ^{1}H (top) and ^{13}C (bottom) spectra of **Ind-BP** in $CDCl_3$ at 298 K.

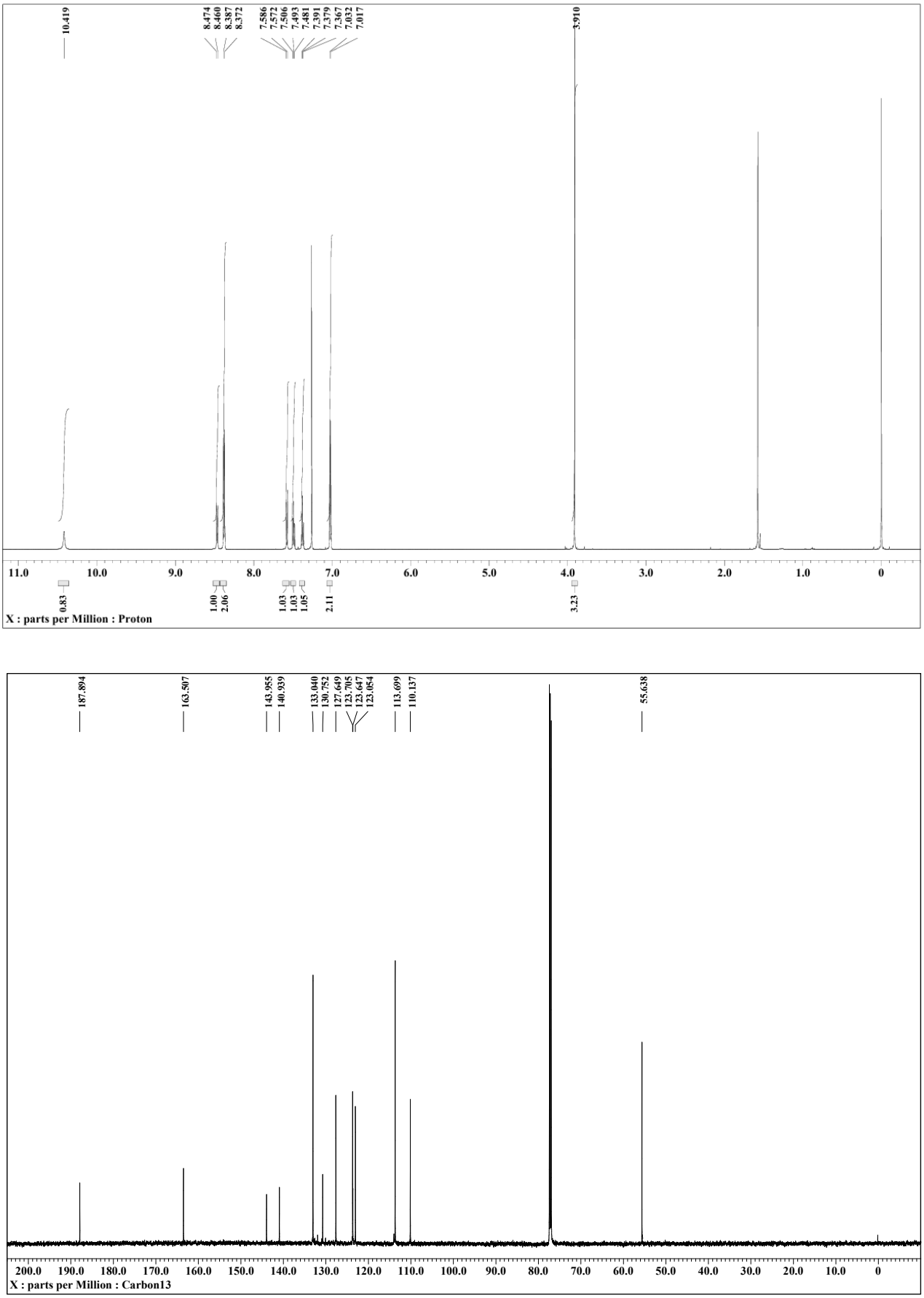

Fig. S9 ^{1}H (top) and ^{13}C (bottom) spectra of **Ind-MP** in $CDCl_3$ at 298 K.

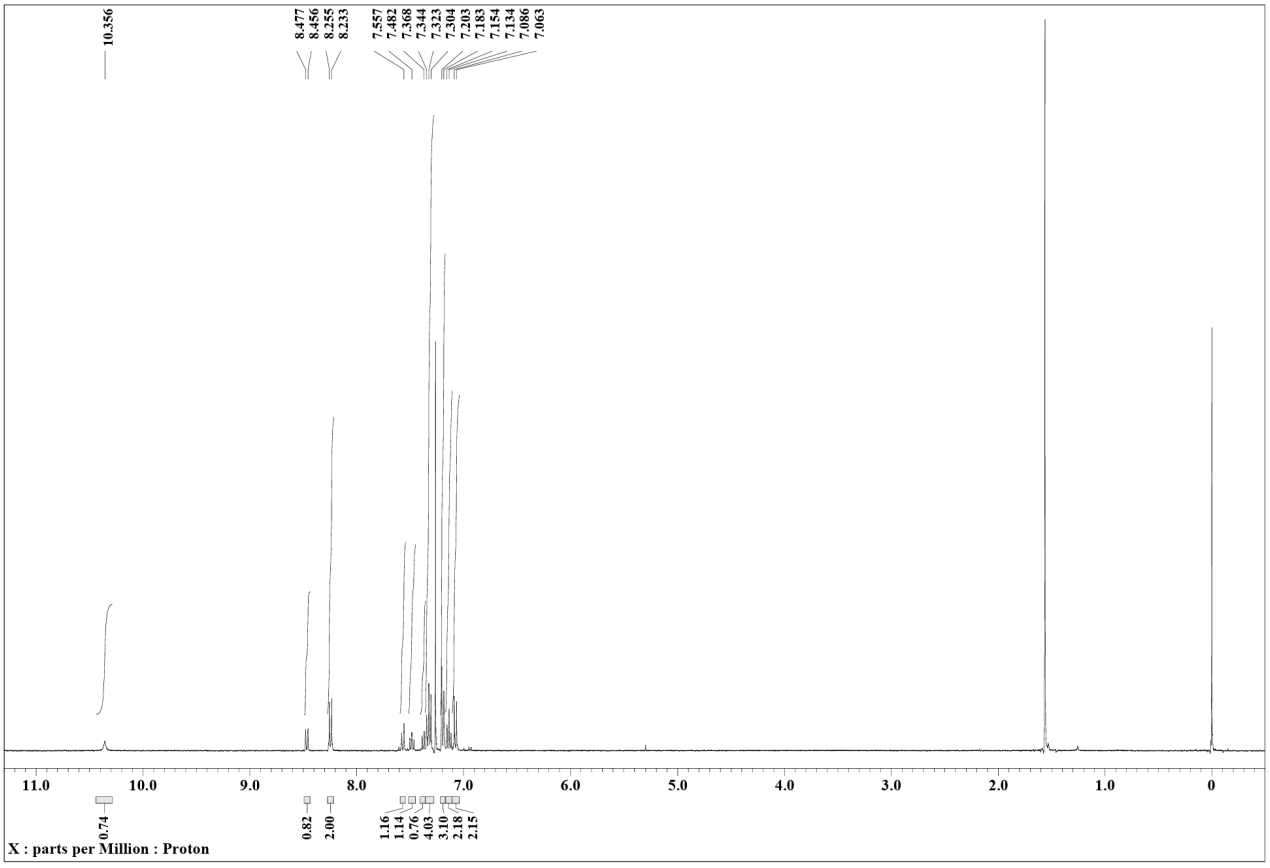

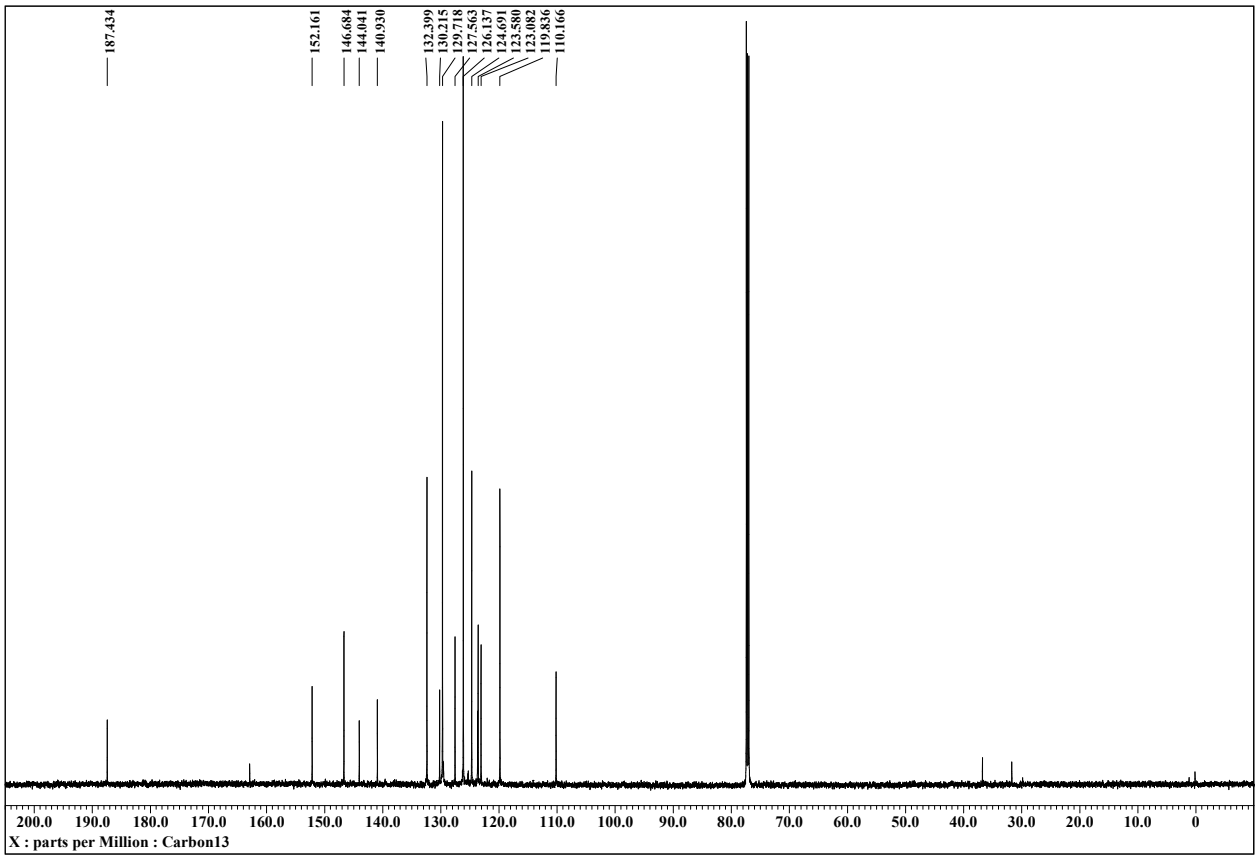

Fig. S10 ^{1}H (top) and ^{13}C (bottom) spectra of **Ind-TPA** in $CDCl_3$ at 298 K.

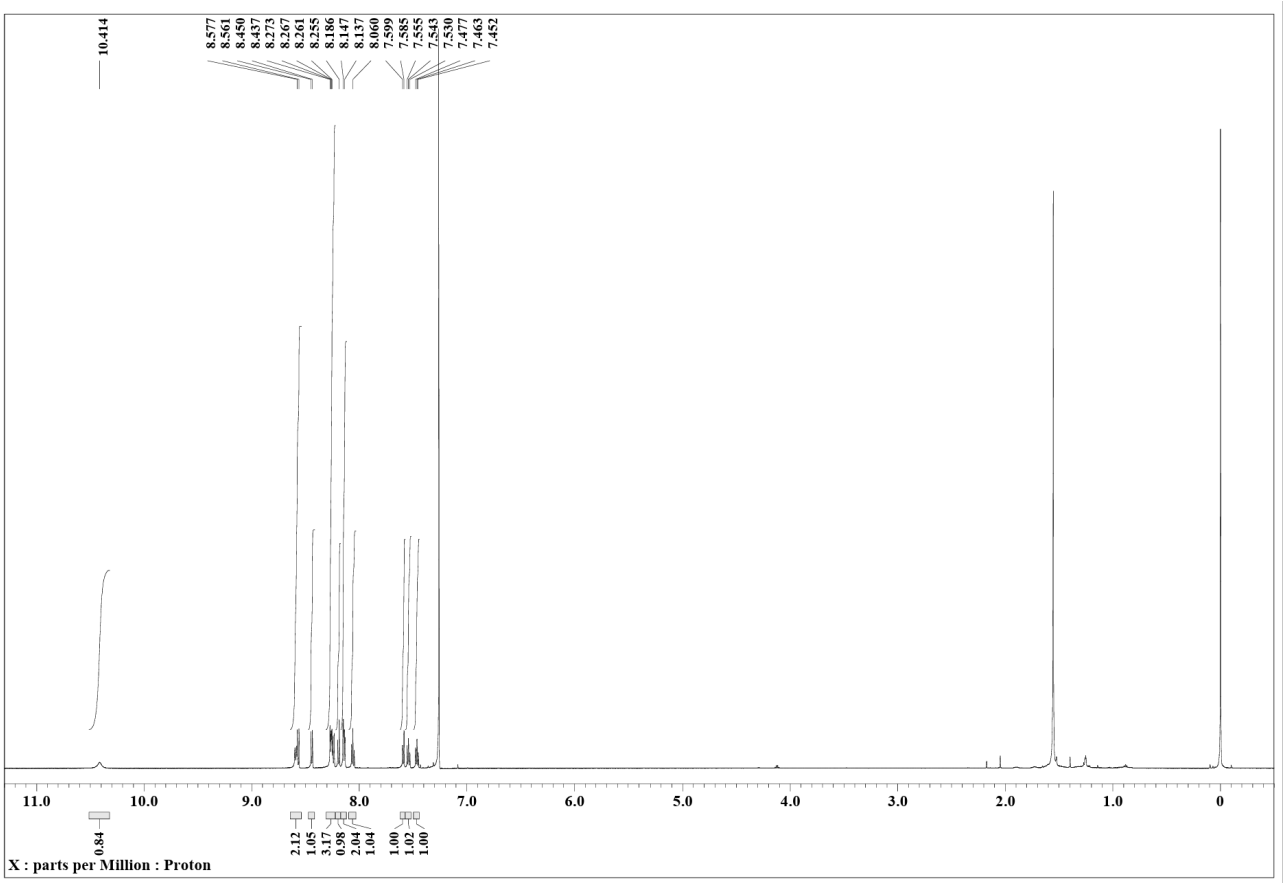

Fig. S11 ^{1}H NMR spectrum of **Ind-Pyr** in $CDCl_3$ at 298 K.

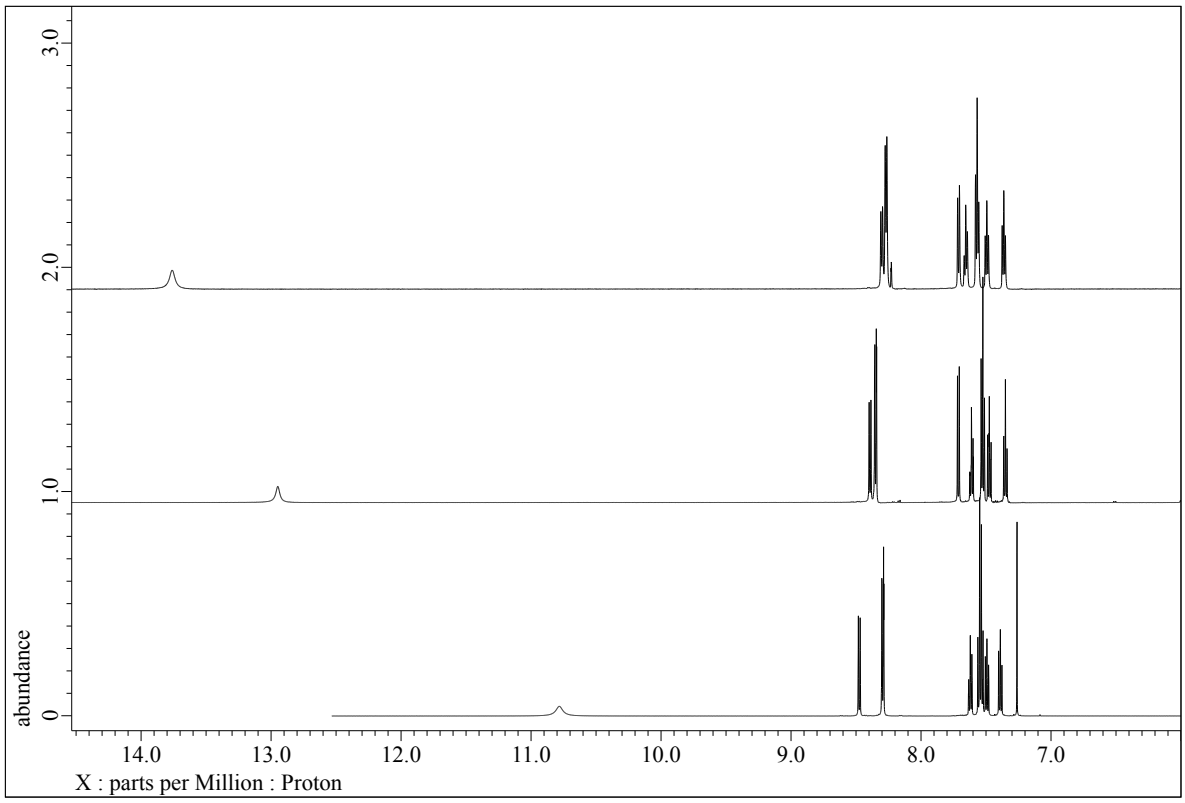

Fig. S12 ^{1}H NMR spectra of **Ind-Ph** in DMSO-d_6 (top), acetone-d_6 (middle), and $CDCl_3$ (bottom) at 298 K.

2. X-ray crystallographic data

Method for single-crystal X-ray analysis: Crystallographic data are summarized in Table S1. A single crystal of **Ind-TPA** was obtained from ethyl acetate/hexane by vapor diffusion method. The data crystal was a green plate of approximate dimensions 1.50 mm × 0.88 mm × 0.10 mm. Data was collected at 150 K on a Rigaku RAPID II diffractometer or a Saturn724R diffractometer with a Mo Ka source. The structures were refined by a full-matrix least-squares method by using a SHELXL 2014[S1] (Yadokari-XG)[S2]. In each structure, the non-hydrogen atoms were refined anisotropically. CIF files (CCDC-2365317) can be obtained free of charge from the Cambridge Crystallographic Data Centre via www.ccdc.cam.ac.uk/data_request/cif.

Table S1 Crystallographic detail for **Ind-TPA**.

	Ind-TPA
formula	$C_{52}H_{38}N_6O_2$
fw	778.88
crystal size, mm	1.50 × 0.88 × 0.10
crystal system	Triclinic
space group	*P*-1 (no. 2)
a, *Å*	8.0437(2)
b, *Å*	13.0080(3)
c, *Å*	18.6634(3)
α, °	87.033(2)
β, °	87.389(2)
γ, °	84.729(2)
V, Å^3	1940.30(8)
ρ_{calcd}, g cm^{-3}	1.333
Z	2
T, K	150(2)
μ, mm^{-1}	0.083
no. of reflns	50330
no. of unique reflns	9852
variables	541
λ, Å	0.71073
R_1 ($I > 2\sigma(I)$)	0.0455
wR_2 ($I > 2\sigma(I)$)	0.1137
GOF	1.065

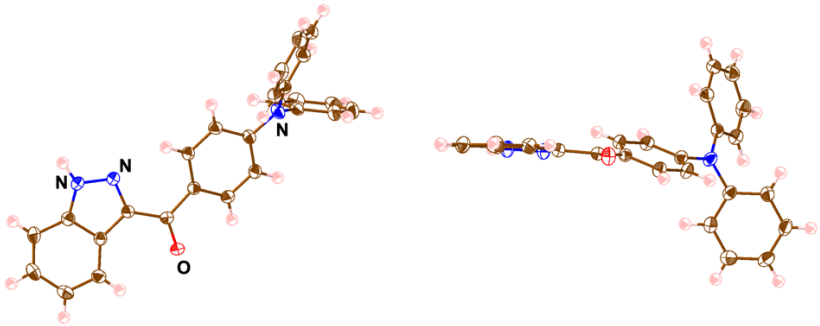

Fig. S13 Ortep drawing of single-crystal X-ray structure (top and side views) of **Ind-TPA**. Thermal ellipsoids are scaled to the 50% probability level. Atom color code: gray, green, blue, and red refer to carbon, hydrogen, nitrogen, and oxygen respectively.

3. Optical properties

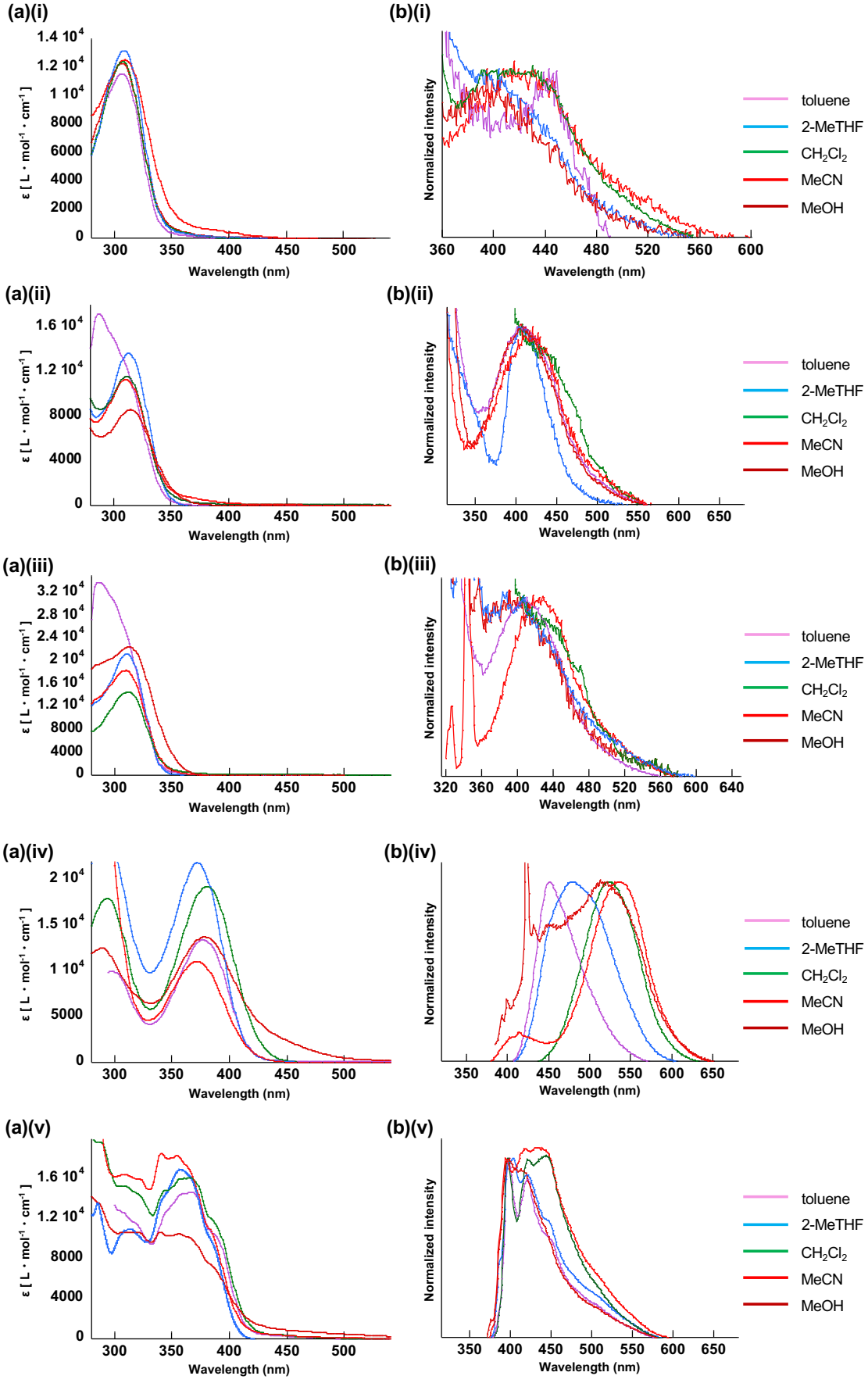

Fig. S14 (a) UV/vis absorption and (b) fluorescence spectra of (i) **Ind-Ph**, (ii) **Ind-BP**, (iii) **Ind-MP**, (iv) **Ind-TPA**, and (v) **Ind-Pyr** in toluene (purple), 2-MeTHF (blue), CH_2Cl_2 (green), MeCN (red), and MeOH (dark red) (10^{-5} M).

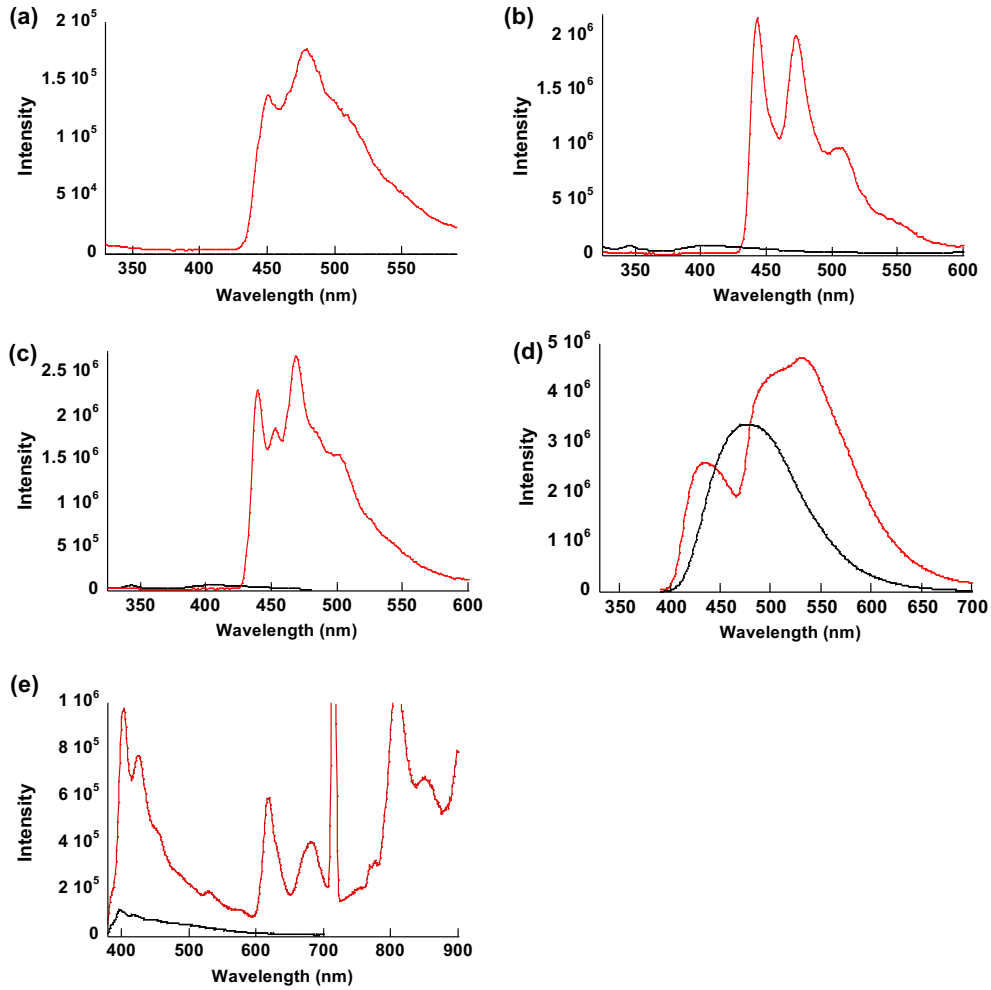

Fig. S15 Emission spectra of (a) **Ind-Ph**, (b) **Ind-BP**, (c) **Ind-MP**, (d) **Ind-TPA**, and (e) **Ind-Pyr** at 298 K (black) and 80 K (red) in 2-MeTHF (10^{-5} M).

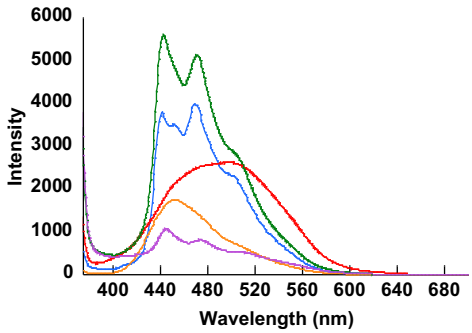

Fig. S16 Emission spectra of Indazole-matrix powder samples (0.1 wt%) for **Ind-Ph** (blue), **Ind-BP** (purple), **Ind-MP** (green), **Ind-TPA** (orange), and **Ind-Pyr** (red) at 298 K. Phenyl benzoate (PhB) was used as matrix. The fluorescence spectra were obtained by excitation at the absorption maximum. The similar fluorescence spectra were obtained by excitation at other absorption bands.

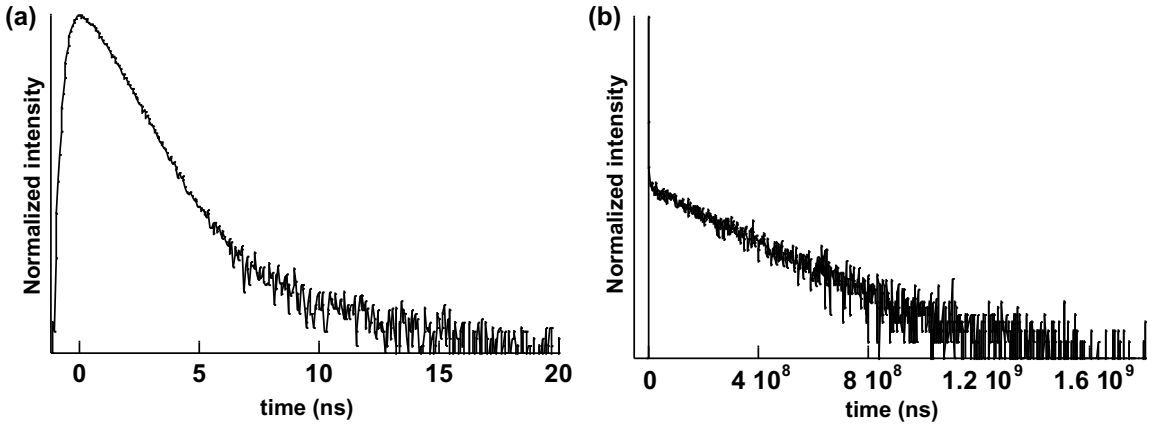

Fig. S17 PL decay curves of **Ind-Ph** in 2-MeTHF (10^{-5} M) monitored at (a) 408 nm (298 K) and (b) 565 nm (80 K).

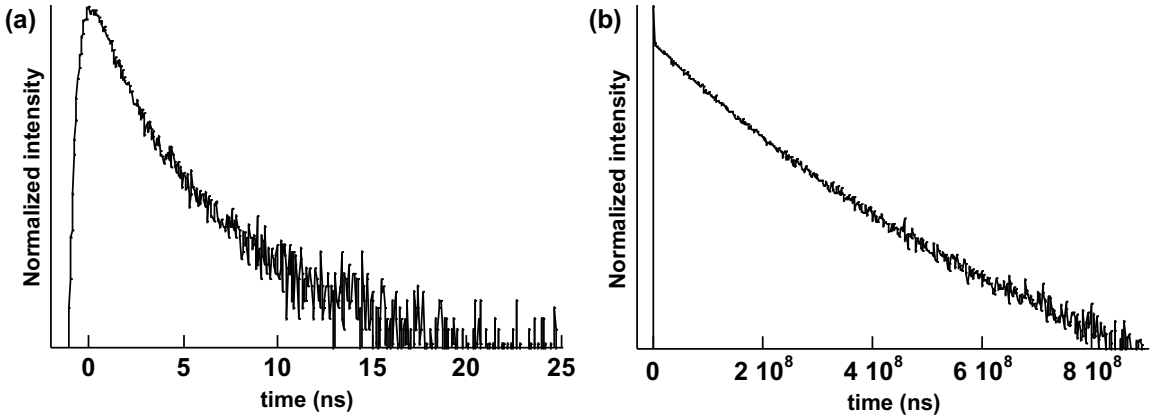

Fig. S18 PL decay curves of **Ind-BP** in 2-MeTHF (10^{-5} M) monitored at (a) 402 nm (298 K) and (b) 472 nm (80 K).

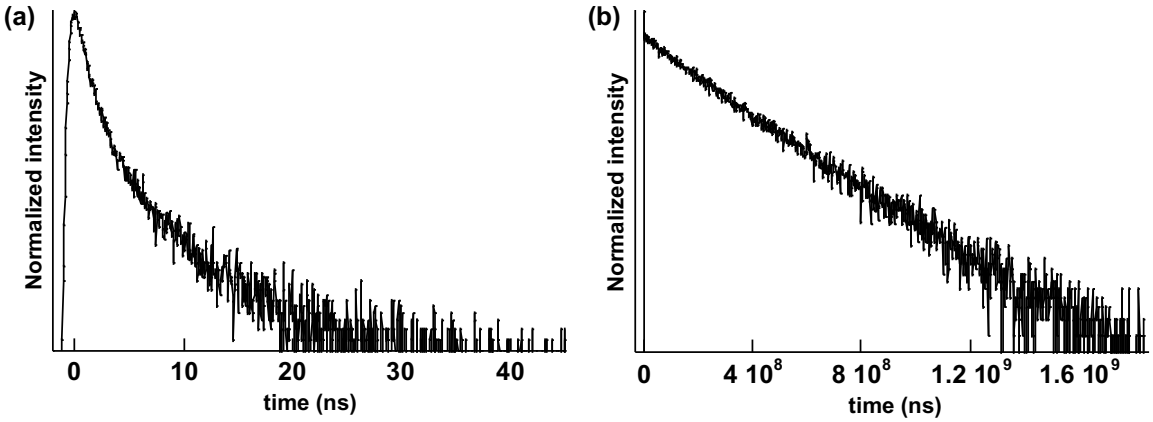

Fig. S19 PL decay curves of **Ind-MP** in 2-MeTHF (10^{-5} M) monitored at (a) 403 nm (298 K) and (b) 468 nm (80 K).

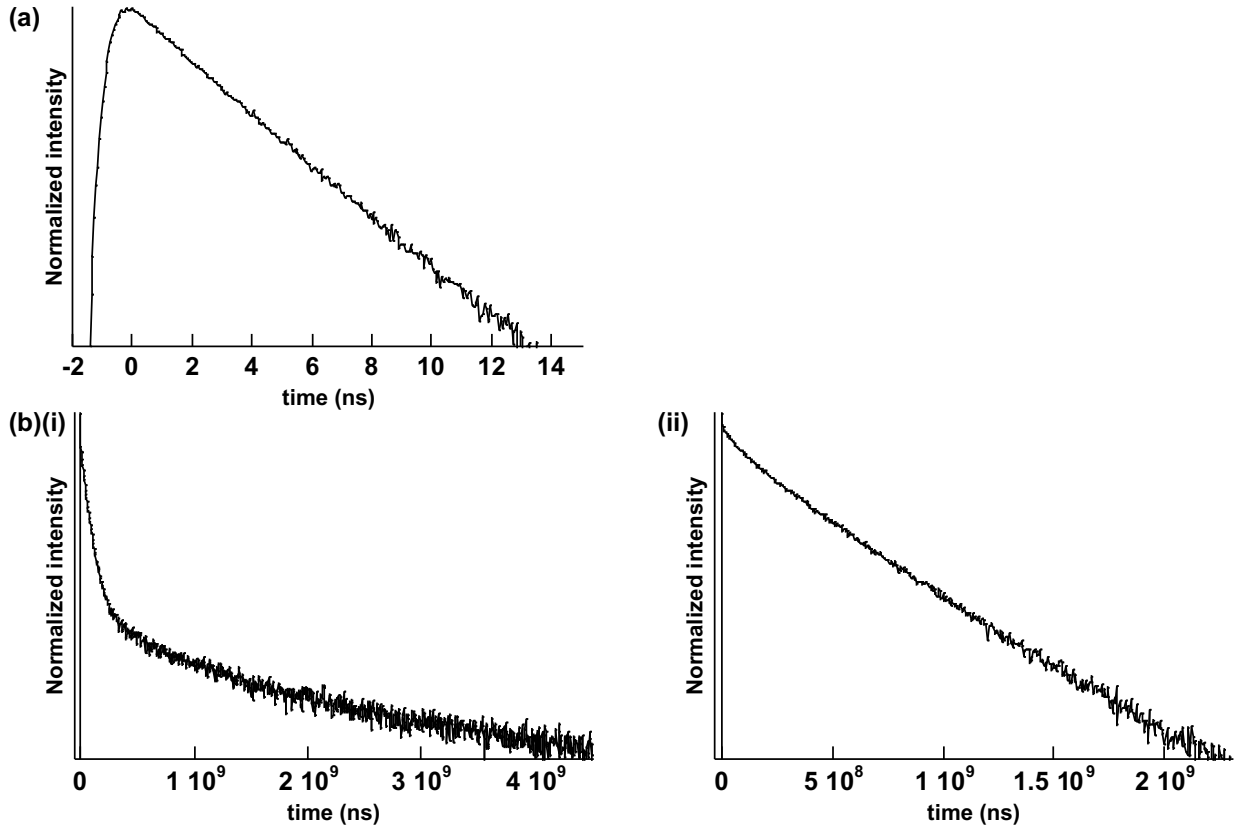

Fig. S20 PL decay curves of **Ind-TPA** in 2-MeTHF (10^{-5} M) monitored at (a) 470 nm (298 K), (b)(i) 434 nm, and (ii) 531 nm (80 K).

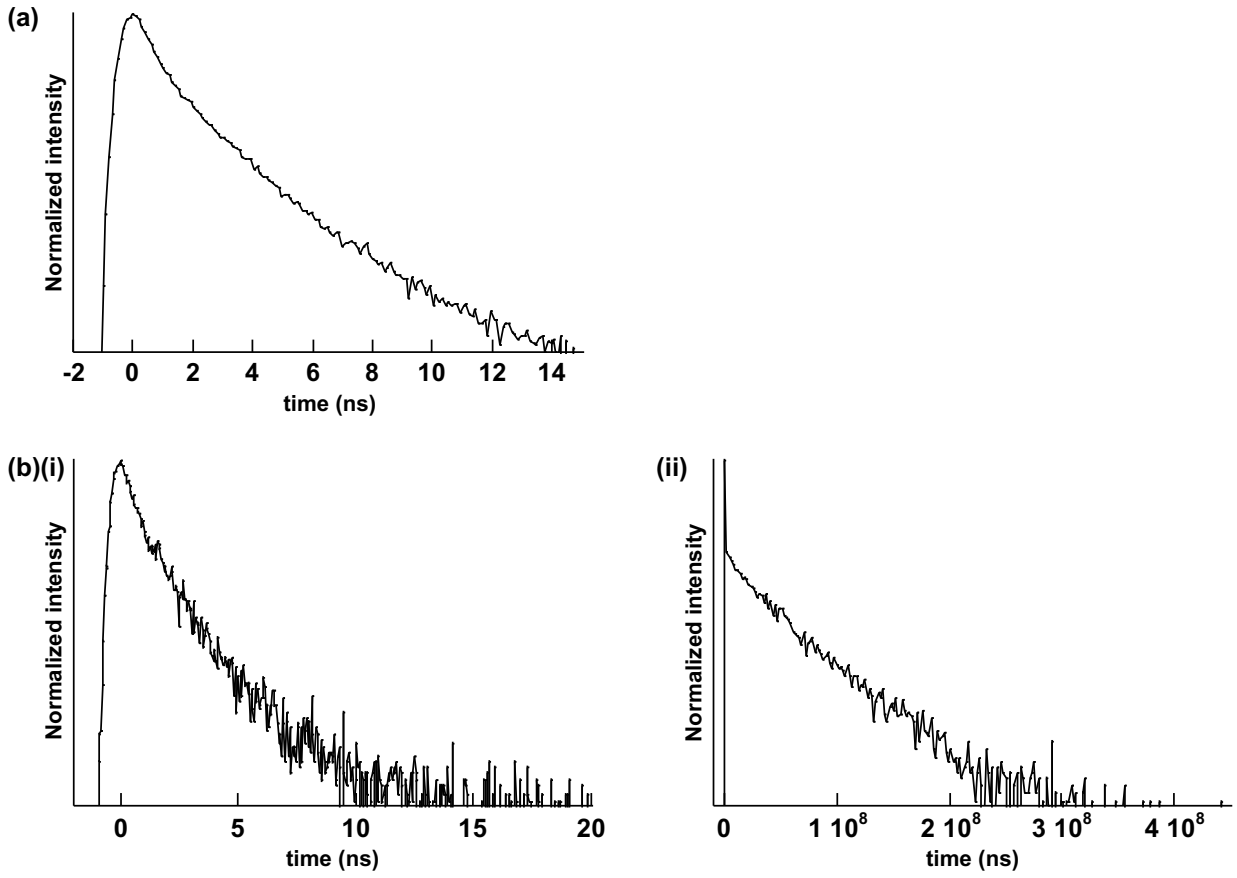

Fig. S21 PL decay curves of **Ind-Pyr** in 2-MeTHF (10^{-5} M) monitored at (a) 403 nm (298 K), (b)(i) 404 nm, and (ii) 619 nm (80 K).

Table S2 Summary of the fitting parameters for the PL decay components. The fitted decay times (τ) of **Ind-Ph**, **Ind-BP**, **Ind-MP**, **Ind-TPA**, and **Ind-Pyr**. (See Fig. S17–21).

	temp.	τ_{ave} (ns)	τ_1 (ns)	τ_2 (ns)	τ_3 (ns)	λ_{ex} (nm)	λ_{em} (nm)
Ind-Ph	298K	11.54	3.136	11.67		340	403
	80K	3.075×10^9	8.377×10^6	3.076×10^9		340	479
Ind-BP	298K	21.37	10.73	45.42		340	402
	80K	1.310×10^9	3.407×10^6	0.7718×10^9	1.582×10^9	340	472
Ind-MP	298K	24.94	10.57	56.04		340	403
	80K	2.800×10^9	7.898×10^6	2.854×10^9		340	468
Ind-TPA	298K	22.40	6.295	24.37		340	470
	80K	3.337×10^9	9.250×10^7	1.326×10^9	3.789×10^9	340	531
	80K	5.789×10^9	3.002×10^7	6.4190×10^8	1.013×10^{10}	340	434
Ind-Pyr	298K	20.82	3.837	20.06	67.44	340	403
	80K	4.876×10^8	4.627×10^6	5.356×10^8		340	619
	80K	25.28	14.06	73.14		340	404

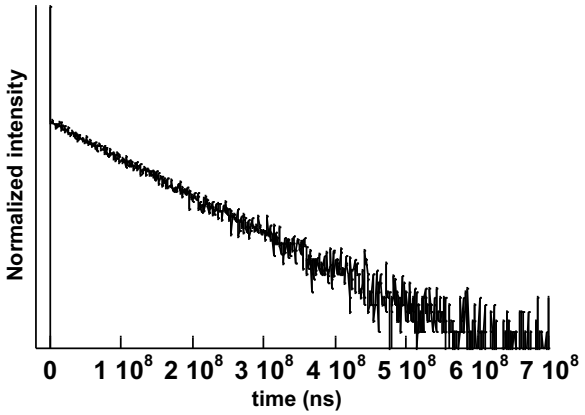

Fig. S22 PL life spectra of **Ind-Ph**–PhB monitored at 565 nm (298 K).

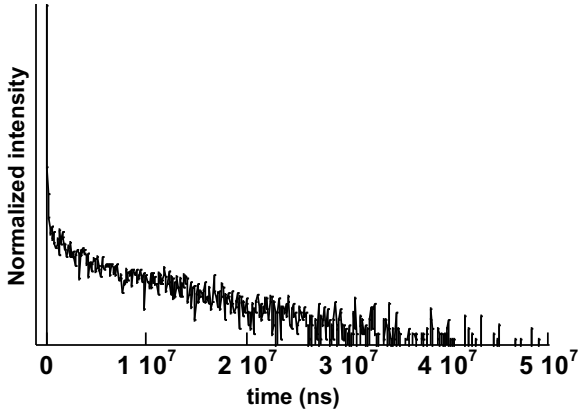

Fig. S23 PL life spectra of **Ind-BP**–PhB monitored at 472 nm (298 K).

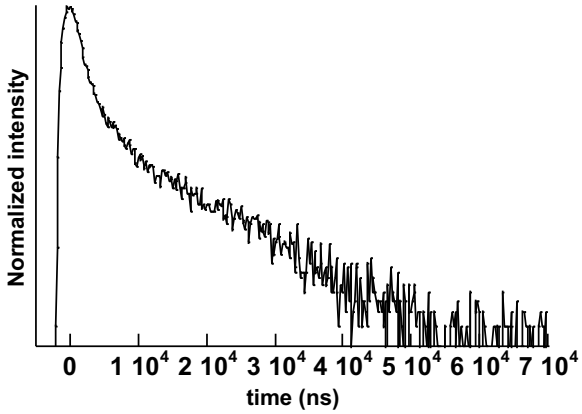

Fig. S24 PL life spectra of **Ind-MP**–PhB monitored at 468 nm (298 K).

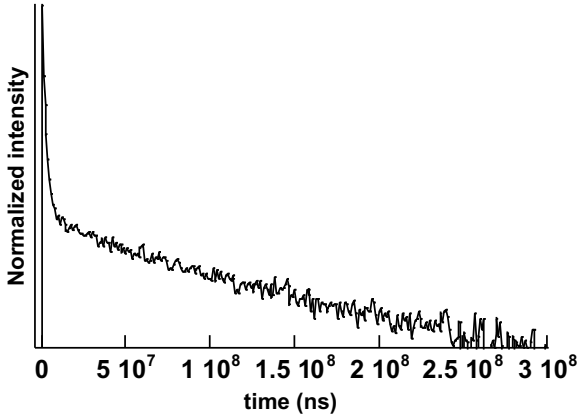

Fig. S25 PL life spectra of **Ind-TPA**–PhB monitored at 531 nm (298 K).

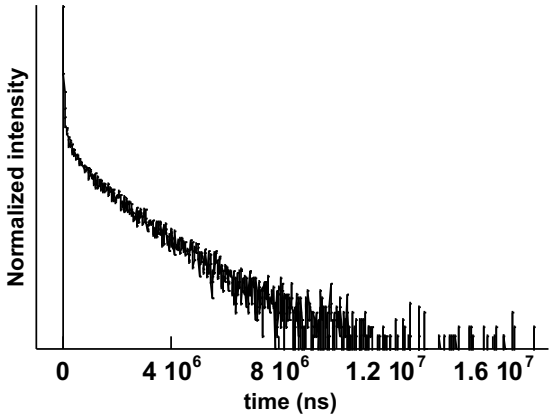

Fig. S26 PL life spectra of **Ind-Pyr**–PhB monitored at 619 nm (298 K).

Table S3 Summary of the fitting parameters for the PL decay components. The fitted decay times (τ) of **Ind-Ph**–PhB, **Ind-BP**–PhB, **Ind-MP**–PhB, **Ind-TPA**–PhB, and **Ind-Pyr**–PhB. (See Fig. S22–26).

	τ_{ave} (ns)	τ_1 (ns)	τ_2 (ns)	τ_3 (ns)	λ_{ex} (nm)	λ_{em} (nm)
Ind-Ph–PhB	1.065×10^9	6.680×10^3	1.066×10^9		340	470
Ind-BP–PhB	7.305×10^7	2.119×10^5	1.314×10^8		340	472
Ind-MP–PhB	1.211×10^6	5.630×10^3	5.260×10^4	5.251×10^6	340	468
Ind-TPA–PhB	5.947×10^8	2.151×10^6	1.624×10^7	1.048×10^9	340	531
Ind-Pyr–PhB	1.474×10^7	5.000×10^4	1.522×10^6	1.963×10^7	340	619

4. Theoretical calculations

Computational method: The calculations were performed using the Gaussian 16 program.[S2] Unless stated, all the structures are confirmed to be minimum-energy structures with no imaginary frequencies.

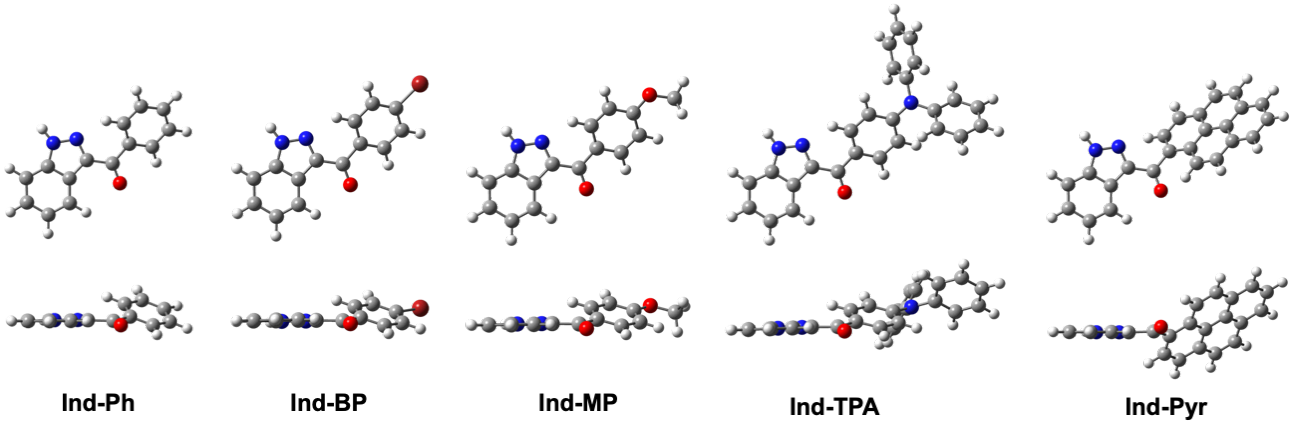

Fig. S27 Optimized structures of **Ind-Ph**, **Ind-BP**, **Ind-MP**, **Ind-TPA**, and **Ind-Pyr** at B3LYP/6-31+G(d) level.

Table S4 Calculated total energies for 1*H*-**Ind-Ph** (E_{1H}) and 2*H*-**Ind-Ph** (E_{2H}) forms of **Ind-Ph** in various solvents. (PCM-B3LYP/6-31+G(d))

	$CDCl_3$	acetone	DMSO
1*H* form (hartree)	–724.2842951	–724.2810775	–724.2881855
2*H* form (hartree)	–724.2774426	–724.2804803	–724.2810775
$E_{2H} - E_{1H}$ (kcal/mol)	4.30	4.43	4.46

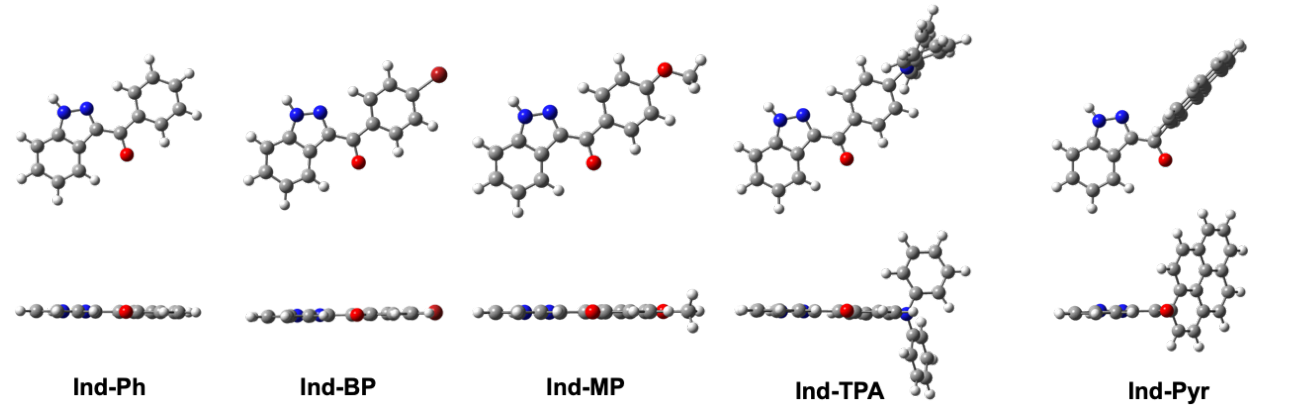

Fig. S28 Optimized structures of **Ind-Ph**, **Ind-BP**, **Ind-MP**, **Ind-TPA**, and **Ind-Pyr** at the S_1 state at TDA-B3LYP/6-31+G(d) level.

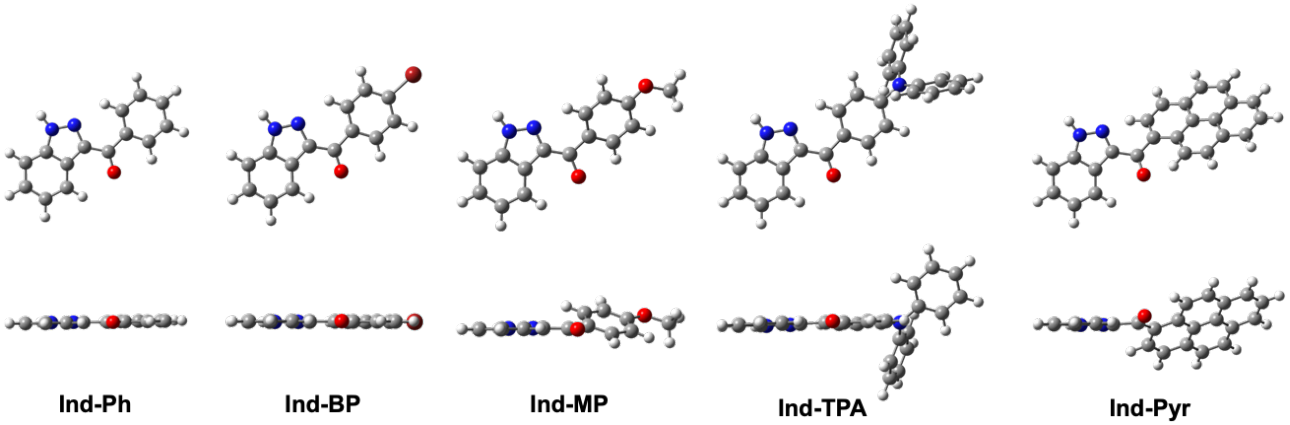

Fig. S29 Optimized structures of **Ind-Ph**, **Ind-BP**, **Ind-MP**, **Ind-TPA**, and **Ind-Pyr** at T_1 state TDA-B3LYP/6-31+G(d) level.

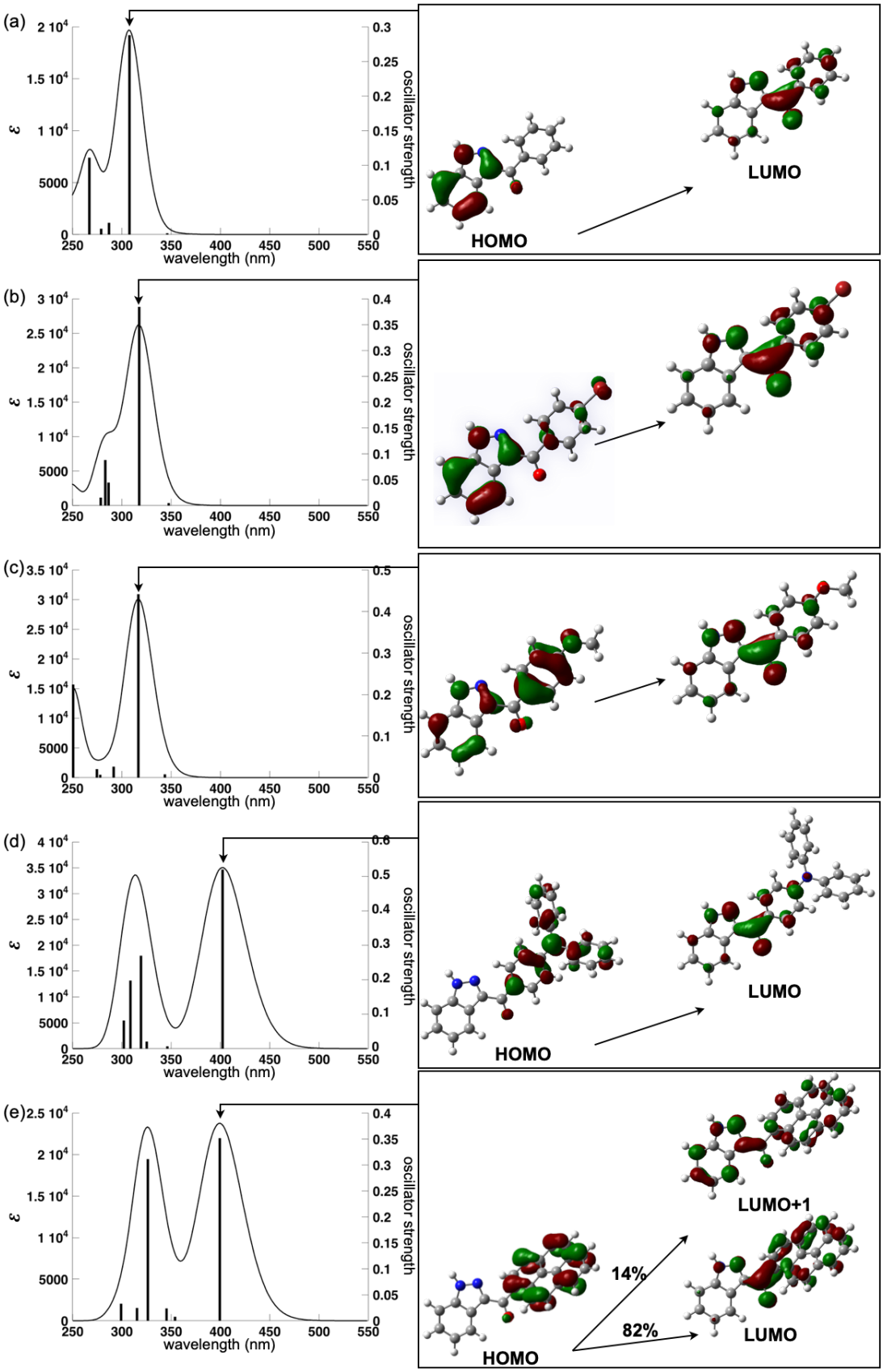

Fig. S30 TD-DFT-based UV/vis absorption stick spectra of **Ind-Ph**, **Ind-BP**, **Ind-MP**, **Ind-TPA**, and **Ind-Pyr** with the transitions correlated with molecular orbitals estimated at B3LYP/6-31+G(d).

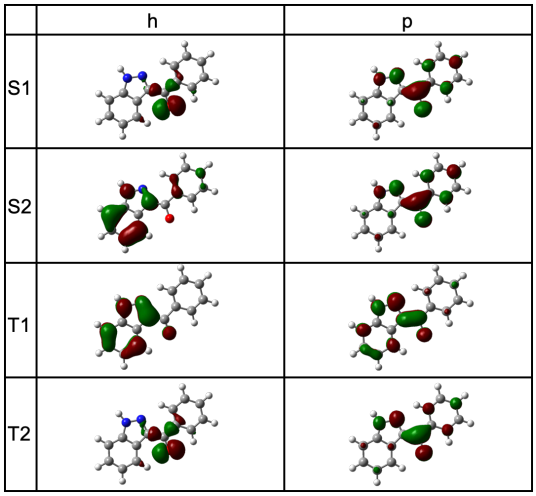

Fig. S31 Natural transition orbitals (NTO) images of the S_1, S_2, T_1, and T_2 excited states of **Ind-Ph**. The NTO images of each excited states represent for their transition forms from the "hole" unity to the "particle" unity, respectively.

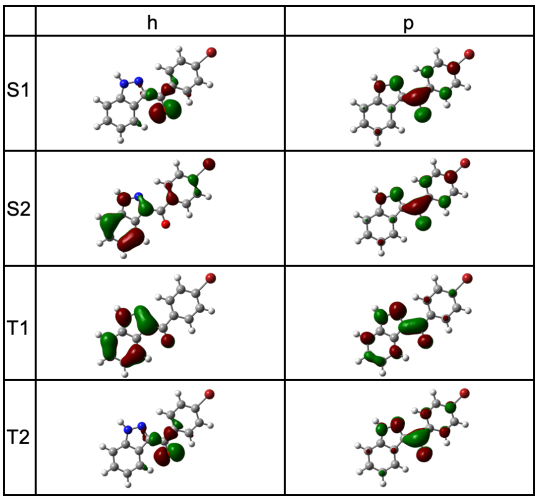

Fig. S32 Natural transition orbitals (NTO) images of the S_1, S_2, T_1, and T_2 excited states of **Ind-BP**. The NTO images of each excited states represent for their transition forms from the "hole" unity to the "particle" unity, respectively.

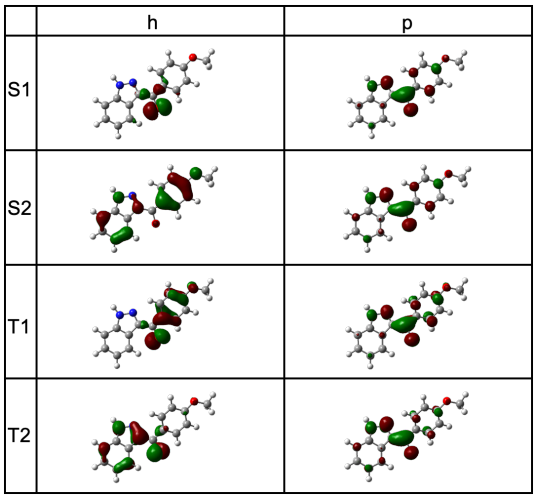

Fig. S33 Natural transition orbitals (NTO) images of the S_1, S_2, T_1, and T_2 excited states of **Ind-MP**. The NTO images of each excited states represent for their transition forms from the "hole" unity to the "particle" unity, respectively.

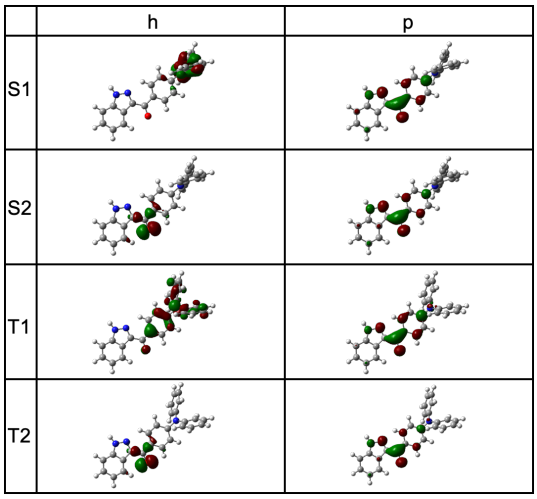

Fig. S34 Natural transition orbitals (NTO) images of the S_1, S_2, T_1, and T_2 excited states of **Ind-TPA**. The NTO images of each excited states represent for their transition forms from the "hole" unity to the "particle" unity, respectively.

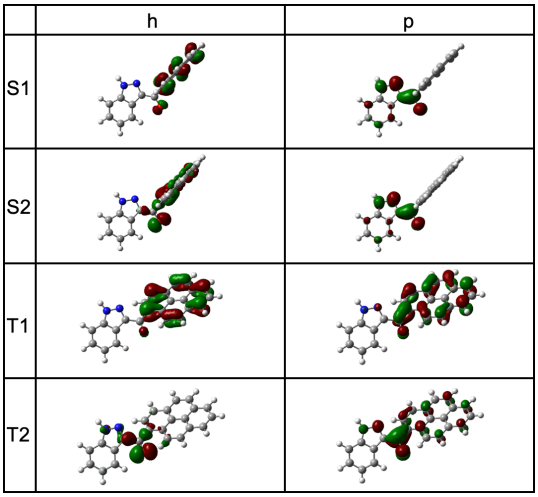

Fig. S35 Natural transition orbitals (NTO) images of the S_1, S_2, T_1, and T_2 excited states of **Ind-Pyr**. The NTO images of each excited states represent for their transition forms from the "hole" unity to the "particle" unity, respectively.

[S1] Sheldrick, G. M., Acta Crystallogr. Sect. A: Found. Crystallogr. 2008, 64, 112-122.
[S2] Wakita, K. Yadokari-XG, Software for Crystal Structure Analyses, 2001.
[S3] M. J. Frisch, G. W. Trucks, H. B. Schlegel, G. E. Scuseria, M. A. Robb, J. R. Cheeseman, G. Scalmani, V. Barone, G. A. Petersson, H. Nakatsuji, X. Li, M. Caricato, A. V. Marenich, J. Bloino, B. G. Janesko, R. Gomperts, B. Mennucci, H. P. Hratchian, J. V. Ortiz, A. F. Izmaylov, J. L. Sonnenberg, D. Williams-Young, F. Ding, F. Lipparini, F. Egidi, J. Goings, B. Peng, A. Petrone, T. Henderson, D. Ranasinghe, V. G. Zakrzewski, J. Gao, N. Rega, G. Zheng, W. Liang, M. Hada, M. Ehara, K. Toyota, R. Fukuda, J. Hasegawa, M. Ishida, T. Nakajima, Y. Honda, O. Kitao, H. Nakai, T. Vreven, K. Throssell, J. J. A. Montgomery, J. E. Peralta, F. Ogliaro, M. J. Bearpark, J. J. Heyd, E. N. Brothers, K. N. Kudin, V. N. Staroverov, T. A. Keith, R. Kobayashi, J. Normand, K. Raghavachari, A. P. Rendell, J. C. Burant, S. S. Iyengar, J. Tomasi, M. Cossi, J. M. Millam, M. Klene, C. Adamo, R. Cammi, J. W. Ochterski, R. L. Martin, K. Morokuma, O. Farkas, J. B. Foresman, D. J. Fox, Revision A.03 ed., Gaussian, Inc., Wallingford CT, **2016**.